

Electrons in high- T_c compounds: *Ab initio* correlation results

Gernot Stollhoff

Max-Planck-Institut für Festkörperforschung, Heisenbergstraße 1, D-70569 Stuttgart, Germany

(Received 14 May 1998)

Electronic correlations in the ground state of an idealized infinite-layer high- T_c compound are computed using the *ab initio* method of local ansatz. Comparisons are made with the local-density approximation results, and the correlation functions are analyzed in detail. These correlation functions are used to determine the effective atomic-interaction parameters for model Hamiltonians. On the resulting model, doping dependencies of the relevant correlations are investigated. Aside from the expected strong atomic correlations, particular spin correlations arise. The dominating contribution is a strong nearest-neighbor correlation that is Stoner enhanced due to the closeness of the ground state to the magnetic phase. This feature depends moderately on doping, and is absent in a single-band Hubbard model. Our calculated spin-correlation function is in good qualitative agreement with that determined from the neutron-scattering experiments for a metal. [S0163-1829(98)03339-6]

I. INTRODUCTION

The theoretical understanding of the microscopic electronic properties of the high- T_c compounds is still incomplete. The only *ab initio* methods that so far have been applied to these compounds are based on the local-density approximation (LDA) within the framework of the density-functional formalism.^{1,2} These fail to describe some of the basic properties like the magnetic transition or the magnetic correlations (for a review see Ref. 3). Consequently, simplified models have been used that are mostly restricted to a single band of strongly correlated electrons, and show a Mott-Hubbard localization transition at half-filling. These seem to explain some of the magnetic properties but their microscopic connection to the full Hamiltonian has not yet been fully established (for a review see Ref. 4).

Here, we present the first application of the local ansatz (LA) to these materials. The LA is an *ab initio* method for the treatment of the correlated electronic ground states of solids.^{5,6} It contains no homogeneous-electron-gas-like approximation whatsoever, and consequently has no problems in overlooking magnetism. The LA yields not only ground-state energies or densities but also detailed correlation functions. In particular, we present the detailed intraplanar correlation features relevant for all high- T_c compounds. Of specific interest are the magnetic correlations. We compare the frequency integrated momentum dependent inelastic magnetic neutron scattering intensity measured for $\text{La}_{0.85}\text{Sr}_{0.15}\text{Cu}_2\text{O}_4$ (Ref. 7) to the LA results and connect it to a specific correlation.

The LA is similar to quantum chemistry (QC) methods, which provide a satisfying description of electrons in small molecules. It allows us to extend the QC accuracy to solid calculations. Like most of these methods, the LA adds correlations as corrections to a single-particle self-consistent-field (SCF) ground state obtained from a Hartree-Fock (HF) calculation where the electrons are described in a restricted single-particle basis of Gaussian-type orbitals (GTO's). The HF computation for the solid is performed by the program CRYSTAL92.⁸ At present, the LA is the only *ab initio* correlation scheme available that makes use of this HF program. Unlike the QC methods, the LA allows a quantitative treat-

ment of electronic correlations for solids, independent of their nature, i.e., whether they are insulators or metals. The LA can do so because it does not attempt to cover the complete spaces of one- or two-particle excitation operators as QC methods usually do, but considers the local character of the relevant correlations from the very outset. It can be seen as an appropriate generalization of the Jastrow ansatz⁹ to inhomogeneous systems.

Every correlation operator in the LA scheme has a very specific meaning. It is constructed from pairs of local orbitals, each of which is connected with a single atom. Consequently, all of the incorporated correlation corrections are separated into those on single atoms and those between atom pairs. The full correlation treatment can be segmented and partitioned with the individual atoms as the smallest available subunit. The correlation operators and their treatment are essentially independent of the nature of the SCF ground state, i.e., whether this be metallic or otherwise. Such a restrictive choice for correlation operators leads to a strong reduction in the correlation-operator space and thus substantially facilitates computations. Necessarily, it admits a small loss of the correlation energy available in a full treatment within a given basis set. From previous calculations, this loss is known to be only 2%, independent of the system size.⁶

The LA was used before for extended molecules such as C_{60} ,¹⁰ three-dimensional semiconductors,¹¹ and ionic insulators,¹² as well as one-dimensional (polyacetylene¹³), two-dimensional (graphite¹⁴), and three-dimensional metals [Li (Ref. 15)]. The calculations presented in this work concern the first application of the LA to a metallic transition-metal compound.

The *ab initio* results also can be used to derive model Hamiltonians that are based on atomic degrees of freedom. The *ab initio* correlation functions obtained from the LA allow us in particular, to unequivocally determine the model interaction parameters.¹⁶ This feature enables us to extend correlation calculations to problems that are still out of reach for *ab initio* LA calculations, and further to make comparisons to models determined by other methods. This is particularly relevant to the high- T_c compounds, the properties of which are often addressed by means of model calculations.

Models based on atomic degrees of freedom consist of selected sets of orthogonalized atomic orbitals i that are related by hopping terms. The interaction part of the Hamiltonian, H_{int}^{mod} , is usually restricted to local interactions

$$H_{int}^{mod} = \sum_i U_i n_{i\uparrow} n_{i\downarrow} \quad (1)$$

for two electrons in the same orbital i . Each interaction-energy parameter U_i dominantly influences a particular correlation function of the correlated ground state Ψ_{corr} for such a model, namely, $\langle \Psi_{corr} | n_{i\uparrow} n_{i\downarrow} | \Psi_{corr} \rangle$, or equivalently the change of this correlation function due to correlations,

$$\Delta_i(\text{corr}) = \langle \Psi_{corr} | n_{i\uparrow} n_{i\downarrow} | \Psi_{corr} \rangle - \langle \Psi_{SCF} | n_{i\uparrow} n_{i\downarrow} | \Psi_{SCF} \rangle. \quad (2)$$

Here, Ψ_{SCF} represents the SCF ground state of the model. As for the *ab initio* treatment, the model ground state is also computed by means of the LA. $\Delta_i(\text{corr})$ equals zero for $U_i = 0$ and rises continuously with U_i . When multiplied with U_i , it is a measure of the interaction energy. This is the relevant relative quantity, when symmetry is broken due to the atomic interactions, and a magnetic or structural phase transition occurs. In such a case, states are compared that differ in those atomic fluctuations. These energy costs due to local charge fluctuations are also relevant in the context of Compton scattering, secondary, or shake up peaks in photoemission or core spectroscopy. For the transition metals, it turns out that the same model interactions are needed for the description of all these properties.^{17–20}

With the unequivocally defined orthogonalized atomic orbitals available in the *ab initio* calculation (see Sec. II), this same correlation function can be determined from the *ab initio* calculation. The model interaction U_i can thus be fixed by demanding that the corresponding model correlation corrections $\Delta_i(\text{corr})$ agree to the same *ab initio* quantities. This connection can also be used to analyze screening details entering such a model interaction. By adding stepwise particular screening contributions in the *ab initio* calculations, we will determine how the model interaction arises, starting from the bare Coulomb interaction. Such an investigation was in the past performed for π -electron interactions in organic compounds.¹⁶

For the high- T_c materials, *ab initio* correlation functions have not yet been available. Model interactions, however, have been computed from the LDA calculations in a different approximation, by freezing specific charges on individual atoms and relaxing the environment. For the most extended model that has been used in this context, a three-band model, the two interaction parameters, namely, an effective local interaction U_d between the $\text{Cu}3d$ -electrons, and an interaction U_p between the $\text{O}2p$ electrons have been obtained in this way.^{21–23} These interactions have then been used to extend the LDA calculations to magnetic properties [by means of the so-called LDA+ U method or by the self-interaction correction (SIC) calculations].²⁴ Model calculations based on these interactions yield photoemission results that are in very good agreement with experiment.²⁵ This agreement is in contrast to the case of, in particular, the middle of the transition-metal series where effective interactions obtained by the LDA do not match the interactions needed for the description

of the above-mentioned properties of these systems (for a comparison, see Ref. 16). For the high- T_c compound that we shall deal with, we will make a comparison between the effective interactions obtained by the LA and by the LDA. It is the first of its kind because for the systems treated so far by the LA no LDA interactions are available. The comparison will shed additional light on the transition-metal case.

For simpler single-band models, interactions have so far been mostly guessed, or obtained by means of fits to specific experiments. Often, they are deduced from the LDA three-band models. However, usually the strong interaction found by the LDA is the only transferred quantity. The $\text{Cu}3d_{x^2-y^2}$ occupation of 1.5 of the LDA (Ref. 24) was usually replaced by occupations smaller than 1.2.⁴ Only under such conditions, a Mott-Hubbard scenario applies.²⁶

This paper is organized as follows. In Sec. II, a short description of the LA and of its possible shortcomings in connection with its application to high- T_c compounds is given. Section III contains a detailed discussion of the *ab initio* computation and an analysis of the correlation functions. These calculations are performed for an idealized high- T_c compound, the so-called infinite-layer system. Wherever possible, comparison to the LDA results is made. Sections IV and V deal with the computation of the model interactions. The former section contains, in particular, a detailed account of the screening mechanisms for the $3d$ transition-metal interaction. In Sec. VI, the dependencies of the most important correlation features on band filling are investigated. This analysis is made on the model level. The *ab initio* program CRYSTAL92 that is used for the SCF calculation is restricted to integer electron occupations per unit cell, and a small change of band filling on the *ab initio* level would demand large unit cells. Finally in Sec. VII, a comparison to neutron-scattering results for a metallic compound is made, and the experimentally found inelastic scattering is connected to a particular correlation obtained by the LA calculation. A summary of our work is presented in the concluding Sec. VIII.

II. COMPUTATIONAL DETAILS

The aim of the paper is a quantitative understanding of the electronic correlations relevant to all high- T_c compounds, namely, those in the individual CuO plane. To simplify the computations, the idealized compound SrCuO_2 is treated. It is a so-called infinite layer compound with CuO planes separated by layers of Sr ions. In the planes, the Cu atoms form a quadratic net with a separation of 3.925 Å, with the O atoms at equal distances between neighbor Cu atoms. The stacking distance, and the perpendicular Cu separation amounts to 3.43 Å. The Sr ions have equal distance to four Cu atoms in the two neighbor planes each. This compound has the smallest possible unit cell containing four atoms. The uppermost valence band is half filled. Therefore, the compound is expected to order antiferromagnetically. Our interest, however, is in the correlations in the metallic state. To represent a doped metallic compound would require a very much larger unit cell. Instead, the metastable nonmagnetic state for the small unit cell is used as a starting point. This approximation is justified because it is known from LDA calculations that the energy bands and Fermi surface of the

metastable half-filled metallic state are very close to the ones for the true metallic compounds.^{3,27}

In a first approximation, this metastable metallic state is obtained from a restricted, non-symmetry-broken Hartree-Fock calculation for this compound, performed with the *ab initio* program CRYSTAL92.⁸ For the Cu and O atoms, good all-electron-GTO-basis sets are used. For Cu, this is a modified (14,11,6) Ahlrichs basis,²⁸ contracted to (6,4,2) orbitals. From the original basis, the outermost diffuse functions were removed, and the next exponents adjusted and reoptimized. For O this is a (11,7) Huzinaga basis,²⁹ the outermost exponents of which were contracted as was done before,^{11,12} plus a set of d orbitals. While the basis sets for the atoms in the planes are of good quality and promise results for the valence electrons close to the Hartree-Fock limit, this is not the case for the Sr atoms. The latter are represented by a large core pseudopotential and a single $5s$ orbital.³⁰ Here, the outermost diffuse basis orbital also was removed. There is no need for such a treatment, but due to this choice, the charge distribution and correlation analysis can be definitely restricted to the degrees of freedom within the plane.

From the SCF calculation, the metallic single-particle ground state $|\Psi_{\text{SCF}}\rangle$ is obtained. Its Fermi surface is identical to that of a LDA calculation for the same compound.²⁷ Also the uppermost energy band is similar to the equivalent LDA band, except for an additional homogeneous spreading by almost a factor of 2 due to the nonlocal and nonscreened exchange. The nonlocal exchange also causes the lower-lying bands to be more separated from the uppermost half-filled band than in the LDA calculation. A presentation of such HF bands, obtained in a somewhat different basis, is found in Ref. 31.

In a next step, correlations are added by the LA. Here, the following variational ansatz is made for the correlated ground state:

$$|\Psi_{\text{corr}}\rangle = e^{-S} |\Psi_{\text{SCF}}\rangle, \quad (3)$$

$$S = \sum_{\nu} \eta_{\nu} O_{\nu} \quad (4)$$

$$O_{\nu} = \begin{cases} n_{i\uparrow} n_{i\downarrow} \\ n_{i\uparrow} n_{j\downarrow} \\ \vec{s}_i \cdot \vec{s}_j \\ \{n_{i\uparrow}(a_{i\downarrow}^{\dagger} a_{j\downarrow} - a_{j\downarrow}^{\dagger} a_{i\downarrow})\} + \{\uparrow \leftrightarrow \downarrow\} \\ n_i \end{cases} \quad (5)$$

The η 's serve as variational parameters. The $n_{i\sigma}$ and \vec{s}_i are density and spin operators for an electron in the local state $a_{i\uparrow}^{\dagger}$, represented by the orbital

$$g_i(\vec{r}) = \sum_j \gamma_{ij} f_j(\vec{r}), \quad (6)$$

where the $f_i(\vec{r})$ are the (GTO-like) basis orbitals. The operators have an obvious meaning. The first operator $n_{i\uparrow} n_{i\downarrow}$, for example, when applied to $|\Psi_{\text{SCF}}\rangle$, projects out all configurations with two electrons in orbital $g_i(\vec{r})$. In connection with the variational parameter η_{ν} , as in Eq. (4), it partially suppresses those configurations. Similarly, the operators $n_i n_j$

describe density correlations between electrons in local orbitals $g_i(\vec{r})$ and $g_j(\vec{r})$. For the homogeneous electron gas, an ansatz with these two kinds of operators leads to the Jastrow function.⁹ The operators $\vec{s}_i \cdot \vec{s}_j$ generate spin correlations. The fourth kind of operator is of the form of $[O_{\nu}, H_0]_{-}$, where H_0 represents the single-particle Hamiltonian. In comparison to the first three kinds of operators, which look like particular interaction contributions, these operators refine the ansatz with respect to the band energy of the electrons involved.⁶ Within the computation, the original operators of Eq. (5) are modified by subtracting the contracted contributions in each of them. The corrected operators when applied to $|\Psi_{\text{SCF}}\rangle$ contain only two-particle excitations, and the corrected, last kind of operator in Eq. (5) covers local single-particle excitations, i.e., it allows for changes in occupations.

The variational parameters η_{ν} are chosen to optimize the energy,

$$E_G = \frac{\langle \Psi_{\text{corr}} | H | \Psi_{\text{corr}} \rangle}{\langle \Psi_{\text{corr}} | \Psi_{\text{corr}} \rangle}, \quad (7)$$

$$= \langle \Psi_{\text{corr}} | H | \Psi_{\text{corr}} \rangle_c. \quad (8)$$

In the last equation, the subscript c indicates that only connected diagram contributions are summed up. This expression cannot be evaluated exactly. The standard approximation is an expansion in powers of η , up to second order,

$$E_G = E_{\text{SCF}} + E_{\text{corr}}, \quad (9)$$

$$E_{\text{corr}} = - \sum_{\nu} \eta_{\nu} \langle O_{\nu}^{\dagger} H \rangle, \quad (10)$$

$$0 = - \sum_{\nu} \eta_{\nu} \langle O_{\nu}^{\dagger} H \rangle + \sum_{\nu, \mu} \eta_{\nu} \eta_{\mu} \langle O_{\nu}^{\dagger} H O_{\mu} \rangle_c. \quad (11)$$

Here, $\langle A \rangle$ means the expectation value of the operator A within $|\Psi_{\text{SCF}}\rangle$. This approximation works only if the correlations are sufficiently weak. Disregarding the reduced subspace of correlation operators, the approximation used so far corresponds to a linearized coupled cluster singlet and doublet (LCCSD) treatment.³² It can be extended to a CCSD treatment.³³

The local orbitals in Eq. (6) are connected to a single atom only and are built from its basis orbitals. This is the essential approximation of the LA.

In the present application, only atomic orbitals are constructed. These are uniquely determined from the SCF ground state by the condition that they are built from basis orbitals on the respective atoms only and that they contain a maximal part of the occupied space. The resulting orbitals are next Löwdin orthogonalized to each other. More localized subatomic orbitals that are usually included in applications of the LA are not used in this first application for a metallic high- T_c compound. Therefore, only interatomic correlations are treated, i.e., correlations that are described by operators built from the atomic orbitals. Shorter-range or intra-atomic correlations, as well as particular polarization correlations, are not covered. From previous experience, it is known that such contributions are not very relevant for the

topics of interest here. Estimated corrections due to the omitted correlations will be given where they are nonnegligible.

In the LA, the correlations are taken into account incrementally. The correlation energy is exactly expressed as an incremental sum over contributions from different sets of atom clusters,

$$E_{\text{corr}} = \sum_{m=1}^N \frac{1}{m!} \times \left\{ \sum_{j_1}^N \sum_{j_2}^N \dots \sum_{j_m}^N \langle E_{\text{corr}}(A_{j_1} A_{j_2} \dots A_{j_m}) \rangle_i \right\}, \quad (12)$$

with $j_1 \neq j_2 \neq \dots \neq j_m$,

where the A_{j_n} denote atoms, on and between which correlation operators are formed and it holds that, for example,

$$\begin{aligned} \langle E_{\text{corr}}(A_1 A_2) \rangle_i \\ = E_{\text{corr}}(A_1 A_2) - E_{\text{corr}}(A_1) - E_{\text{corr}}(A_2), \end{aligned} \quad (13)$$

i.e., the increments $\langle \rangle_i$ include only the changes of the correlation energy due to the extended set represented. Translation invariance and the particular local symmetry are easily included by performing the above summation only over the subset of symmetry inequivalent clusters. For every computation, the exact solid single-particle expectation values are taken.

For the coverage of the interaction part, the local nature of the correlation operators allows a drastically simplifying reduction. In a finite basis set per atom representation, the interaction is represented by a fourth-order tensor of basis interaction matrix elements the indices of which extend over the involved basis orbitals. The generation of this tensor and its handling are the limiting steps in a correlation calculation. For the particular correlations on the set of atoms treated, the required tensor can, to a very good approximation, be restricted to these atoms plus all their nearest neighbors. This restriction makes all required computations easily feasible. Possible corrections due to lacking matrix elements are included in computations extending over larger clusters. The two largest clusters for which explicit *ab initio* correlation calculations were performed are depicted in Fig. 1. The larger one consists of five active Cu atoms and four active O atoms. The basis interaction matrix elements are computed for the whole Cu_5O_{16} cluster. As will be demonstrated, the most relevant information can be satisfactorily obtained from correlation calculations extending up to this size of clusters.

Two approximations made for the handling of the LA need further discussion in connection with the application to a high- T_c compound. The one is the restriction to weak correlations while the high- T_c compounds are usually connected with a Mott-Hubbard transition. The LCCSD approximation, in which the LA is computed, fails for the strongly correlated half-filled band case. However, it does so in a controllable way. For too strong correlations, the correlation corrections turn too large and lead to negative density correlation functions. The criterion of positive density correlations can be taken as an indication as to whether the LA results are still meaningful. Away from half-filling, the LA behaves better, and for an almost empty band, it applies even for diverging

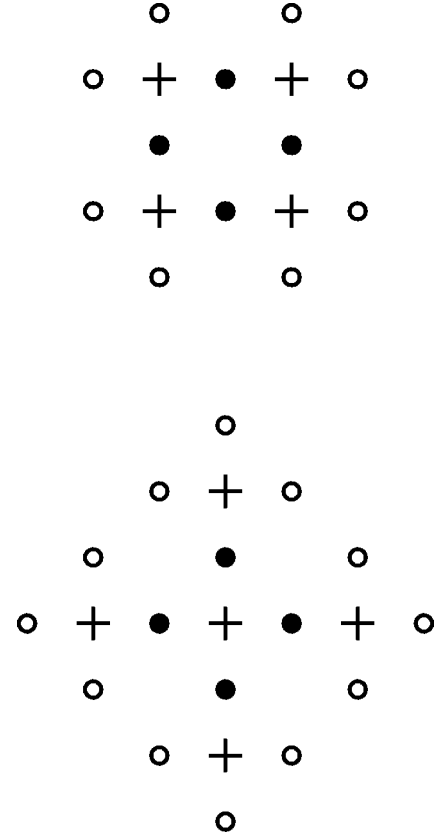


FIG. 1. Schematic representation of the two largest clusters for which interaction matrix elements for the basis orbitals were generated. Cu atoms are denoted by crosses, O atoms for which correlation operators were included are denoted by filled circles, while O atoms that contributed only to the V_{ijkl} are denoted by open circles.

interaction. Also, a more quantitative test can be made. Individual correlation corrections such as the one due to a single correlation operator $n_{i\uparrow}n_{i\downarrow}$ can be computed variationally, i.e., exactly. Here, a comparison with the result of Eq. (11) in the same operator subspace can be made, and the overestimation of the correlation expansion can be quantified. Such a variational calculation restricting to two-particle excitations has no meaning for the treatment of the full extended system (N) due to lack of size consistency. The resulting correlation energy would scale like \sqrt{N} . When such a variational computation is extended to more than a single operator, it can only give a lower limit to the correlation results. Earlier *ab initio* calculations with the LA for finite Cu-O clusters³⁴ and experience with successful LA model calculations for the transition metals themselves^{35,17,18} have already indicated that the range of applicability of the LA might well extend to the high- T_c materials.

The second approximation made is the restricted SCF ground state that is used as a starting point, although the particular system chosen is known to be antiferromagnetically ordered. The LCCSD approximation is sensitive to antiferromagnetic order. This is in contrast to standard perturbation expansions, and can be seen by resolving the LCCSD equation (11), leading to

$$E_{\text{corr}} = - \sum_{\nu\mu} \langle \text{O}_{\nu}^{\dagger} \text{H} \rangle (\langle \text{O}^{\dagger} \text{H} \text{O} \rangle_c)_{\nu\mu}^{-1} \langle \text{O}_{\mu}^{\dagger} \text{H} \rangle. \quad (14)$$

TABLE I. Correlation energy contributions in atomic units for particular successively added operators and relative amount of spin correlations.

Correlations	E_{corr} (a.u./u.c.)	Spin contrib.
On site	-0.1248	
Cu-O nn	-0.0154	0.20
Cu-Cu nn	-0.0190	0.80
O-O nn	-0.0033	
Cu-O nnn	-0.0036	
Cu-Cu nnn	-0.0157	0.95
Cu-Cu nnnn	-0.0040	0.95

The denominator contains the exact two-particle excitation energies. If the restricted SCF ground state turns unstable, its susceptibility diverges for a particular wave vector, and consequently two-particle excited states must exist with energies degenerate to or even lower than the SCF ground-state energy. With sufficiently extended sets of correlation operators, the matrix $\langle\text{OHO}\rangle$ is no more positive definite, and the scheme turns unstable. From such a calculation, also the smallest set of correlation operators may be determined that leads to instability. In particular, a lower limit for the size of stable magnetically ordered domains can be obtained. This holds true as long as the phase transition from the metal to the insulator as a function of occupation is second order. If the transition is first order, then the computation in the metastable metallic state is still relevant for the doped metallic state but might lack information about the magnetic order.

III. RESULTS OF THE CORRELATION CALCULATIONS

We will next present the *ab initio* results of the LA in separate chapters for correlation energies, charge distributions, and particular correlation functions. In all cases, partial correlations are consecutively added, starting from atomic terms, and extending up to the longest-range correlations included, namely, the ones between third-nearest-neighbor Cu atoms.

A. Detailed correlation energies

In Table I, the contributions of the different classes of operators to the correlation energy are displayed. The sets of operators are grouped into those on individual atoms and those between different atoms. For the latter cases, the fraction of spin operator contributions is also given. As expected, the largest overall energy gain is due to the on-site or atomic correlations. Here, the largest part is from the $\text{Cu}3d_{x^2-y^2}$ operators. However, almost 20% of the on-site contributions is connected with a charge transfer that will be discussed in more detail later.

There are two different kinds of relevant longer range contributions. One arises from correlation operators between neighbor Cu and O atoms. Here, no specific contribution is dominating. Rather the very local atomic correlation hole generated by the atomic operators is smoothly extended, adding 10% of the on-site correlation energies. The second kind is connected with spin correlations between different Cu atoms, and, in particular, with those between electrons in the

TABLE II. Charge distributions for the HF ground state and with correlations added, in comparison to LDA results (Ref. 42).

Orbital	HF	On-site corr.	nn corr.	Full corr.	LDA
$\text{Cu}3d_{x^2-y^2}$	1.51	1.33	1.17	1.15	
$\text{Cu}3d_{z^2}$	1.95	1.94	1.94	1.94	9.30*
$\text{Cu}3d_{xy}, 3d_{xz}, 3d_{yz}$	2.00	2.00	2.00	2.00	
$\text{Cu}4s$	0.50	0.55	0.57	0.58	0.53
$\text{Cu}4p_{pl}$	0.30	0.33	0.34	0.34	0.64*
$\text{Cu}4p_{\perp}$	0.09	0.11	0.11	0.11	
$\text{O}2s$	1.82	1.82	1.81	1.81	
$\text{O}2p_b$	1.42	1.48	1.57	1.58	
$\text{O}2p_{orth}$	1.97	1.96	1.96	1.96	
$\text{O}2p_{\perp}$	1.95	1.93	1.92	1.91	

*The sums over five respectively three partial contributions each are given.

$\text{Cu}3d_{x^2-y^2}$ orbitals. These dominate the nearest-neighbor Cu-Cu correlations and are exclusively responsible for the longer-range terms. The neighbor Cu-Cu correlations will later be discussed in more detail. The longer-range correlations are connected with the eventual formation of long-range magnetic order. Next-nearest Cu-Cu contributions to the energy are as large as nearest-neighbor contributions, indicating that here problems with the metastability of the non-magnetic SCF ground state begin to show up.

While all shorter-range correlations were fully or almost completely converged with respect to the series of clusters selected, this does not hold true anymore for the third-nearest-neighbor Cu-Cu contributions. However, divergence does not yet appear. This indicates that stable antiferromagnetic correlations at half-filling need to coherently extend over domains larger than the clusters selected for the correlation computation.

When added, all these correlations represent an energy gain of roughly 5 eV per unit cell. All these correlations are due to binding, and the resulting correlation energy amounts to a large fraction of the total binding energy.

B. Partial charge distributions

The partial charge distributions $n_i(\Psi) = \langle\Psi|\sum_{\sigma}n_{i\sigma}|\Psi\rangle$ are presented in Table II for different states Ψ . The first row contains the values for $\Psi = \Psi_{SCF}$. When added, the partial occupations reach the number of valence electrons up to 0.02. This indicates the good quality of the computed orthogonal atomic orbitals. The occupation of the $\text{Cu}3d$ orbitals is very close to the estimate for the solid, obtained from earlier finite cluster HF calculations,³⁴ except for the $\text{Cu}4s, 4p$ occupations. In the earlier calculation, these came out smaller for two reasons. The one is that a basis set was used that lacked the most extended exponents used here for the $4s, p$ orbitals. This restriction was made to avoid artifacts, resulting from the large negative charging of the small clusters treated. The second reason is that, in the earlier calculation, the $4s$ and $4p$ orbitals were Schmidt orthogonalized to the $\text{O}2s, 2p$ orbitals, while here all orbitals are equally treated by a mutual Löwdin orthogonalization.

With the addition of correlations, a relatively large charge transfer occurs. Ultimately, it is a charge transfer mostly from the $\text{Cu}3d_{x^2-y^2}$ orbitals into the $\text{O}2p$ orbitals. However, for an understanding of this it is necessary to progress stepwise. A first step is the addition of atomic correlations that lead to a large correlation energy gain. The dominant charge transfer due to the atomic correlations is from the $\text{Cu}3d_{x^2-y^2}$ orbitals to the $\text{Cu}4s,4p$ orbitals, followed by a secondary redistribution from the $\text{Cu}4s,4p$ orbitals to the $\text{O}2p$ orbitals. Overall, 0.18 electrons are removed from the $\text{Cu}3d_{x^2-y^2}$ orbitals, and put into the $\text{Cu}4s,p$ shell (0.13) and the $\text{O}2s,p$ shells (2×0.03). This charge transfer was not detected in the earlier cluster calculation for the poor $\text{Cu}4s,p$ basis.³⁴ More than 80% of this charge transfer arise from the inclusion of the operators $n_{i\uparrow}n_{i\downarrow}$ for the $\text{Cu}3d_{x^2-y^2}$ orbitals; the remaining part stems from the same operators for the $4s,p$ orbitals.

This charge transfer due to atomic correlations is closely related to the negative magnetovolume effect known from transition metals as will be shown next. The correlation-induced charge transfer detected here partially corrects an inverse exchange-induced charge transfer. The dominant exchange contribution of relevance in this context is from atomic interactions $U_{at}(i)$ and is written as $E_{at}(\text{exch}) = -\sum_i U_{at}(i)n_{i\sigma}^2(\Psi_{HF})$ where the sum runs over the i atomic orbitals in the unit cell, and $n_{i\sigma}(\Psi_{HF})$ indicates the HF occupation of orbital i per spin. To simplify the discussion, we restrict to two different atomic orbitals, and assume that they have the same interaction U but an occupation $n_{1\sigma}$ very much larger than an occupation $n_{2\sigma}$. A charge transfer z from n_2 into n_1 leads to the exchange energy gain $\Delta E(\text{exch}) = -2zU(n_{1\sigma} - n_{2\sigma})$. Therefore, the HF exchange enhances differences in charge distributions. For the case treated here, the HF exchange is responsible for a charge transfer from the little filled $4s,p$ orbitals into the strongly filled $3d$ orbitals. Also a trend for a similar charge transfer from the $4s,p$ orbitals into the strongly filled $\text{O}2s,p$ orbitals is expected, but should be restricted by Hartree (or essentially Madelung) contributions. The latter terms do not influence intra-atomic charge transfer. No charge transfer between the $\text{Cu}3d$ and $\text{O}2p$ orbitals is expected from atomic exchange as long as these orbitals have a similar occupation and not very different atomic interactions. When on-site or atomic correlations are included, a sizable fraction of the exchange-induced charge transfer is undone. This is the origin of the charge redistribution found in the present computation. Another way to undo the exchange induced charge transfer is to turn the system magnetic. This corresponds to a maximal atomic correlation. Consequently, a charge transfer must come into play when magnetism in systems with very differently filled subshells is concerned, as for the case of itinerant ferromagnetism of the $3d$ metals. For Ni, for example, one would expect a somewhat larger filling of the $3d$ orbitals for the nonmagnetic state than for the ferromagnetic state at the cost of the $4s,p$ occupation, because contrary to the fully magnetic case, the electrons are not completely correlated in the nonmagnetic state, as is well known.¹⁸

Such a charge transfer becomes relevant for the magnetovolume effect. A theoretical description of magnetism that is restricted to a particular shell (like the set of $3d$ orbitals) implies that the antibonding orbitals are more populated in the magnetic case no matter how strong correlations are. In

such a case, the volume always increases with magnetic order. When more than one shell is involved, the just mentioned charge transfer comes into play. For Ni, this is from the bonding $4s,p$ orbitals into the (few and antibonding) empty orbitals of the $3d$ shell. It implies a negative magnetovolume contribution. Ni actually displays a total negative magnetovolume effect.³⁶ The latter cannot be understood within a description restricted to the $3d$ orbitals,¹⁸ but can only be explained by a not fully screened exchange-induced charge transfer. On the HF level, this exchange-induced $3d$ - $4s$ charge transfer was first proposed many years ago as the origin of the negative magnetovolume effect.³⁷

It would be of interest to find out whether also in the case of the high- T_c compounds a negative magnetovolume effect exists. With the new version of the CRYSTAL program,³⁸ which allows for unrestricted HF calculations, such an investigation will become feasible from the theoretical side.

When neighbor correlations are included, then an additional charge transfer of the same magnitude as the one due to on-site correlations occurs. It is dominantly from the $\text{Cu}3d_{x^2-y^2}$ orbitals to the $\text{O}2p_b$ orbitals, and is due to a particular spin correlation between neighbor Cu sites that will be discussed later. The longer-range contributions that were covered by the present computations lead to a further but small transfer of the same kind. A similar but somewhat smaller charge transfer had been found in the earlier finite cluster calculations.³⁴ It should be noted that this secondary charge transfer is connected with a small correlation energy gain.

The exact occupation of the $\text{Cu}3d_{x^2-y^2}$ orbitals is of very much interest. It is directly connected to the measured moment of the magnetic ground state and plays a crucial role for models used for the high- T_c compounds. These usually assume that the occupation of the $\text{Cu}3d_{x^2-y^2}$ orbital is not very different from 1.0. The present calculations indicate that in fact different correlation mechanisms bring the occupation into this range. To validate these findings, a short discussion on the possible deficiencies of the presented computation shall be given next.

While the result of the HF calculation can be assumed to be close to the HF limit, this does not hold true for the correlation treatment. A first possible error is connected with the weak correlation approximation. From the exact treatment of a particular on-site correlation plus the connected charge transfer, it can be estimated that the on-site correlation correction of the $\text{Cu}3d_{x^2-y^2}$ occupation is overestimated by 10–15%. For the charge transfer arising from longer-range correlations, no error estimate can be made. Two further corrections are expected. The one is the influence of shorter than atomic range correlations, the other is the screening particularly of the $3d$ orbitals due to the Cu core—and here especially due to the $3s$ and $3p$ orbitals. Since the calculation presented here is the first *ab initio* correlation calculation ever for a metallic transition-metal compound, no reference results exist. Even comparable detailed calculations for small clusters are lacking. From atomic calculations, some estimate for corrections can be gained. Such corrections are expressed in terms of energy differences. In HF approximation, the excited $3d_94s_2$ state of the Cu atom is 0.4 eV higher than the ground state, while experimentally the difference amounts to 1.5 eV.³⁹ A similar correction is found

when the ground and excited states of the Ni atom are concerned.⁴⁰ This correction is exclusively due to short-range correlations, core polarization effects, and relativistic corrections, none of which were included in the presented calculation. The influence of these corrections to the presented results can be estimated by lowering the diagonal atomic $3d$ energy level by 1 eV. For the model discussed below, this leads to a charge transfer into the $\text{Cu}3d_{x^2-y^2}$ orbitals of roughly 0.05. The lacking short-range correlations alone would have a somewhat larger influence than this total shift but are counterbalanced by relativistic corrections that favor the $4s$ electrons.⁴¹ Adding these corrections, the final estimate for the $\text{Cu}3d_{x^2-y^2}$ occupation amounts to 1.22 ± 0.07 . For reasons discussed above, it is smaller than the value deduced from the earlier cluster calculations.³⁴ Future applications will hopefully reduce the uncertainty in the present LA results.

It is of interest to compare this LA result to an LDA charge analysis. Table II also contains LDA results that were obtained for $\text{YBa}_2\text{Cu}_3\text{O}_{6.5}$.⁴² The latter compound is not a so-called half-filled system, and the respective charge distribution represents a lower limit to the half-filled case. In the referred publication, only integrated occupations for complete shells were given. Also, the underlying charge analysis was performed differently. This might lead to sizable deviations when the more delocalized orbitals are concerned but is hoped to lead to comparable results for the very localized $3d$ orbitals. From the global $3d$ occupation, not much can be concluded about the $\text{Cu}3d_{x^2-y^2}$ occupation. However, an LDA calculation performed for the system treated here at half-filling leads to a $\text{Cu}3d_{x^2-y^2}$ occupation of 1.55,⁴³ and other high- T_c compounds at half-filling are usually mapped by $\text{Cu}3d_{x^2-y^2}$ occupations of 1.5.²⁵ These LDA values are very close to the HF results but differ from the correlation result and from the final estimate.

This deviation of the LDA result from the LA occupation is expected to result from deficiencies of the used homogeneous electron gas approximation. It is plausible to conclude that the specific neighbor Cu spin correlations leading to a charge transfer of 0.17 are not at all covered by the LDA. Such a simple connection cannot be made with respect to the charge transfer caused by on-site exchange terms and the correlation compensations. It is known that the LDA is not able to describe anisotropic exchange contributions. In particular, the LDA is not able to produce the negative magnetovolume effect for Ni.⁴⁴ This indicates that it lacks exchange induced transfer and partial correlation compensation, but no large overall error is expected on the atomic scale. A very rough error estimate of the charge distribution due to LDA deficiencies on the atomic scale can be made using an analysis of LDA results for two-atomic clusters. These indicate that the $3d$ orbitals are too attractive in comparison to the $4s$ orbitals. Expressed in diagonal energies, a correcting shift of 1 eV was computed.⁴⁵ Such an atomic LDA correction is similar in size to the joint correlation/relativistic correction of the HF energy differences for the atoms but has a different prefactor. It leads to a charge transfer of 0.05 out of the $\text{Cu}3d_{x^2-y^2}$ orbital.

Overall, the LDA seems to overestimate the occupation of the $\text{Cu}3d_{x^2-y^2}$ orbitals by roughly 0.3, a large fraction of which is explained. It should be kept in mind, however, that

the atomic orbitals are differently defined in both methods. This causes some uncertainty. In the future, it will be possible, to perform LDA calculations with a new version of the CRYSTAL program,³⁸ and to analyze the results by the LA routines, so that at least this last uncertainty can be removed.

The mutual influence of correlations and charge redistributions is of relevance to *ab initio* methods that try to address correlations with Monte Carlo schemes. Variational Monte Carlo calculations⁴⁶ as well as diffusion Monte Carlo calculations (for a review, see Ref. 47) rely on a good trial state. For the first method, the charge distribution of the trial state is usually frozen to avoid the optimization of very costly external variational parameters, while the second method is restricted by the frozen nodes of the ground-state wave function. The findings of the LA calculation indicate that a better trial state than the so far always selected LDA ground-state wave function might be needed.

C. Atomic correlations

Next, we discuss the individual atomic correlations and their strength. The average occupation of orbital i in the correlated ground state is defined as $n_i = \sum_{\sigma} n_{i\sigma}(\Psi_{\text{corr}})$. The charge fluctuations within orbital i , Δn_i^2 , are given as

$$\begin{aligned} \Delta n_i^2 &= \left\langle \Psi_{\text{corr}} \left| \left(\sum_{\sigma} n_{i\sigma} \right)^2 \right| \Psi_{\text{corr}} \right\rangle - n_i^2 \\ &= n_i \left[1 - \left(\frac{n_i}{2} \right) \right] + 2\Delta_i(\text{corr}) \end{aligned} \quad (15)$$

$$= 2[\Delta_i(\text{HF}) + \Delta_i(\text{corr})]. \quad (16)$$

They are separated into the HF charge fluctuations, $\Delta_i(\text{HF})$, and the correlation corrections $\Delta_i(\text{corr})$ [see Eq. (2)]. The former are defined as the charge fluctuations in a fictitious single-particle state that has the charge distribution of the correlated ground state. These charge fluctuations represent the electronic mobility. For a single-particle state, it holds that

$$\Delta_i(\text{HF}) = \sum_{j \neq i} P_{ij}^2, \quad (17)$$

where P_{ij} represents the density-matrix elements per spin to all other orthogonal atomic orbitals. The kinetic-energy gain due to delocalization of the electrons in this state is proportional to $\sum_{(j)} P_{ij}$, with the summation (j) restricted to nearest neighbors of i . Consequently, the reduction of $\Delta_i(\text{HF})$ due to correlations, $\Delta_i(\text{corr})$, gives also a rough measure of how much band energy is lost by the correlations.

Charge fluctuations can only be completely frozen out for half-filling, i.e., for $n_i = 1.0$. In all other other cases, there is a maximal correlation reduction, $\Delta_i(\text{corr,max})$, which amounts to

$$\Delta_i(\text{corr,max}) = \begin{cases} \left(\frac{n_i}{2} \right)^2 & \text{for } n_i < 1 \\ \left(1 - \frac{n_i}{2} \right)^2 & \text{for } n_i > 1. \end{cases} \quad (18)$$

TABLE III. On-site correlations for the different atomic orbitals. The individual terms are defined in the text.

Orbital	n_i	Δ_i (HF)	Δ_i (corr)	Δ_i (corr, max)
$\text{Cu}3d_{x^2-y^2}$	1.17	0.243	-0.122	-0.172
$\text{Cu}4s$	0.57	0.203	-0.009	-0.081
$\text{Cu}4p_{pl}$	0.34	0.141	-0.005	-0.029
$\text{O}2s$	1.81	0.086	-0.002	-0.009
$\text{O}2p_b$	1.57	0.168	-0.033	-0.049

The relative correlation strength ζ_i is defined as $\zeta_i = [\Delta_i(\text{corr})]/[\Delta_i(\text{corr,max})]$.

All of these quantities are given in Table III for the final result of the correlated ground state. As can be seen, correlations are strongest for the $\text{Cu}3d_{x^2-y^2}$ orbital. Nevertheless, even there, half of the original fluctuations survive, indicating that the electrons are still very delocalized, and that a renormalization of the effective mass due to atomic correlations of no more than 30% is to be expected. Nevertheless, 70% of the possible reductions are realized. Next in strength are the correlations on the $\text{O}2p_b$ orbitals. Also here, the correlation strength is 0.7 although the reductions amount to only 20% of all fluctuation in this orbital. The correlations in all other orbitals are weak. This even holds true for the O_{2s} orbital.

The correlation strength strongly depends on the included correlations. When restricting to on-site correlations, the $\text{Cu}3d_{x^2-y^2}$ occupation is 1.33. Then, it holds that $\Delta_i(\text{corr}) = -0.096$, which represents an 85% reduction. Freezing the $\text{Cu}3d_{x^2-y^2}$ charge at the HF value, i.e., close to the value of the $\text{O}2p_b$ charge, leads to a correlation strength of more than 0.90. This will be explained later when analyzing these correlation functions in the context of model interactions.

A set of trial variational calculations restricted to individual correlation operators was also performed. This was done to control the validity of the variational expansion. When comparing these variational results to the variational expansion results, it was found that the correlations obtained by the expansion calculation were overestimated by 10–15% for the $\text{Cu}3d_{x^2-y^2}$ orbitals, but less than 5% for all other on-site correlations. This small correction indicates that the expansion is fully able to cover these correlations. Consequently, there is no evidence that correlations on the atomic scale are too strong for a weak-correlation expansion treatment.

There are additional corrections expected from the omitted correlations. From earlier calculations for other systems, it was found that the longer-range correlations that were neglected here have no influence on the atomic correlation functions (for a detailed explanation, see, e.g., Ref. 16). The short-range correlations omitted here, however, led to a reduction of the atomic correlation corrections for the $2s,p$ orbitals by $10 \pm 5\%$.¹⁶ Consequently, they are expected to lead to a somewhat larger reduction for the $3d$ orbitals, which are characterized by a somewhat higher average density. When added, a reduced correlation strength of 0.53 ± 0.04 instead of 0.7 is expected for the $\text{Cu}3d_{x^2-y^2}$ orbitals, when an occupation of 1.17 is assumed. Such a correlation

TABLE IV. Spin-correlation functions for $\text{Cu}3d_{x^2-y^2}$ orbitals between neighbor sites $i, i + \nu$, as functions of the included correlation operators, in comparison to the $2d$ Heisenberg model.

Included correlations	$\nu=0$	$\nu=1$	$\nu=2$	$\nu=3$
HF ground state	0.276	-0.012	0.001	0.001
On site	0.478			
Up to $\nu=1$	0.530	-0.140		
Up to $\nu=2$	0.540	-0.220	0.170	
Up to $\nu=3$	0.543	-0.243	0.183	0.072
Heisenberg model	0.75	-0.34	>0.10	>0.10

correction is not terribly large but is rather similar to the correlation strength obtained for the transition metals from model calculations.¹⁷

This correlation strength obtained for the metastable half-filled state should not strongly change when electrons are removed from the planes. Actually, for such a case, the $\text{Cu}3d_{x^2-y^2}$ occupation comes closer to 1.0, and $\Delta_i(\text{corr})$ is expected to increase while ζ_i decreases. Therefore, the results obtained for the half-filled case are expected to be representative for relevant dopings.

Complete magnetic order implies a correlation strength of 1.0. Consequently, we would expect a certain additional charge transfer $3d-4s,p$ with magnetization. This might even lead to a negative magnetovolume effect.

D. Spin correlations

Of particular interest are the spin-correlation functions $S(i,j)$ between the different atomic orbitals (i,j), defined as

$$S(i,j) = \langle \Psi_{\text{corr}} | \vec{s}_i \vec{s}_j | \Psi_{\text{corr}} \rangle. \quad (19)$$

For the on site terms, it holds in general that $S(i,i) = \frac{3}{2}[\Delta_i(\text{HF}) - \Delta_i(\text{corr})]$. For the SCF ground state, these expectation values do not vanish, and represent the autocorrelations of the electrons. They are small except for the on-site terms and the neighbor Cu-O contributions. For the correlated ground state, it turned out that only spin correlations between the $\text{Cu}3d_{x^2-y^2}$ orbitals on the different atoms are relevant. This is in contrast to earlier calculations for small clusters. There, longer-range spin-density-wave-like correlations occurred at which the $\text{O}2p_b$ orbitals participated.³⁴ Apparently, these small clusters rather represented a one-dimensional chain than the intended plane.

Table IV displays the correlations $S(i,j)$, where the indices (i,j) are restricted to $\text{Cu}3d_{x^2-y^2}$ orbitals. These correlation functions are computed incrementally. In a first step, only on-site correlations are included, and only the on-site function is given, then neighbor interactions plus the neighbor functions are successively included. The enhancement of the on-site terms with inclusion of longer-range correlations is due to the enlarged charge transfer.

The antiferromagnetic Cu-neighbor spin correlations are large and are connected with a sizable charge transfer from Cu to O that was discussed above. The coupling of spin correlations to a charge transfer arises because spin correlations are maximal for a $\text{Cu}3d_{x^2-y^2}$ occupation of 1. In more

detail, the quantity most relevant for the spin-correlation strength is the expectation value $\langle \vec{s}_i \vec{s}_j H \rangle$, where i, j represent neighbor $\text{Cu}3d_{x^2-y^2}$ orbitals. The dominant contributions from the Hamiltonian are the on-site interactions on Cu, U_{3d} , and on O, U_{2p} . When restricting ourselves to these interactions, and to the largest density-matrix elements P_{ij} , the above expectation value is given by

$$\langle \vec{s}_i \vec{s}_j H \rangle = \frac{3}{2} [2U_{3d_{x^2-y^2}} n_{i\sigma} (1 - n_{i\sigma}) P_2^2 - U_{2p} P_1^4]. \quad (20)$$

Here, $n_{i\sigma}$ represents the SCF occupation of the Cu orbital per spin, and P_1 the neighbor Cu-O density-matrix element and P_2 the neighbor Cu-Cu density-matrix element. It holds that $n_{i\sigma} > |P_1| > |P_2|$ for the relevant range of occupations. For the half-filled SCF ground state, the first term of Eq. (20) is one order of magnitude larger than the second. The correlation-induced charge transfer results probably because the matrix element $\langle O, H \rangle$ is enhanced by a charge transfer from the Cu orbital to the O orbital. Due to such a transfer, the first part increases, while the second part strongly decreases. The charge transfer stops when the $\text{Cu}3d_{x^2-y^2}$ occupation reaches 1.

The *ab initio* results show that the charge transfer due to the secondary spin correlation is large. This suggests that the ground state must also be relatively unstable with respect to any other external disturbance that profits from such a charge transfer. Perhaps this instability also contributes to the lattice instability, and, in particular, to the large buckling found for this compound.⁴⁸ In view of this sensitivity, it is even more astonishing that the very much larger on-site correlations did not lead to a sizable Cu-O charge transfer.

These neighbor correlations are quite strong, stronger than needed to counterbalance the change in the wave function due to on-site correlations. For a singlet state Ψ it always holds that $\sum_{ij} \langle \Psi | \vec{s}_i \vec{s}_j | \Psi \rangle = 0$. For the SCF ground state, the on-site terms are counterbalanced in part by antiferromagnetic neighbor Cu-O spin correlations, while the remaining correction is rather long range. When correlations up to neighbor Cu atoms are included, then the neighbor Cu-Cu correlations alone more than counterbalance the correlation-enhanced on-site terms. This can be viewed as a quite sizable attraction of electrons of different spin on neighbor sites even in the absence of longer-range antiferromagnetic order. In fact, it will be later demonstrated that these correlations depend little on doping.

While the nearest-neighbor correlations represented in Table IV are converged with respect to the treated cluster sizes (as long as no longer-range correlation operators are added), this does not quite hold true for the second-nearest-neighbor terms. Here, another 10% might be obtained from more extended cluster contributions. Third-nearest neighbors when added are not converged at all. Here a renormalization of at least a factor of 2 is expected from larger clusters.

More extended clusters and longer-range spin correlations were not covered since already the results obtained so far led to spin-correlation corrections that turn out to be too large. This indicates the proximity to the antiferromagnetic instability. In some individual cluster calculations, already next-nearest-neighbor contributions turned out to be almost as large as nearest-neighbor terms. Nevertheless, for the included clusters the expected computation breakdown was not

yet seen. Such a breakdown must arise as soon as a cluster size is reached where in HF approximation a broken symmetry ground state is preferred. Consequently it is concluded that even for the half-filled case antiferromagnetic order parameter fluctuations need to extend over domains that are larger than the cluster explicitly included in the computations.

The longer-range correlations contribute differently from the nearest-neighbor (nn) correlations. The direct coupling matrix elements $\langle O, H \rangle$ are negligible. However, the longer range operators are more sensitive to electrons very close to the Fermi surface. Consequently, spin correlations may form that are dominated by the band electrons very close to the Fermi energy.

It is of interest to compare these correlation functions with those of a two-dimensional Heisenberg model.⁴⁹ For the latter, the on-site and neighbor correlation functions are also given in Table IV together with the long-range limit. It can be seen that the short-range correlation functions of the Heisenberg model are larger than those of the real system. This is because in the real system the $\text{Cu}3d_{x^2-y^2}$ orbitals are more than half filled, and because they are not perfectly correlated. On the other hand, the short-range correlations of the real system extend already beyond the long-range correlation pattern of the Heisenberg model. The limiting correlation function in the magnetically ordered high- T_c materials is typically $\lim_{\nu \rightarrow \infty} |S(i, i + \nu)| = 0.08 - 0.10$.^{49,50} Except for the not yet converged $\nu = 3$ term, this is well below the short-range correlation functions obtained from the present calculation.

IV. DETERMINATION OF A MODEL HAMILTONIAN

The *ab initio* results of the LA provide sufficient information to unequivocally determine a model Hamiltonian. Such a condensation of *ab initio* results to a model serves multiple purposes. One of them is to forward *ab initio* informations to computations that can no more be performed on an *ab initio* level but only for a model. In the following, this applies to the computation of the doping dependency of the properties discussed above that were calculated for half-filling. Due to the restrictions of CRYSTAL92 such *ab initio* calculations would become costly. Another purpose is that information about particular correlations can be represented in the form of effective interactions. Usually, experiments are fitted by models that are represented by the adapted interactions, but no correlation function for the model is computed. Such a connection will facilitate comparisons, also for differing systems. For the case of the high- T_c compounds, finally, the explicit treatment of correlations has been so far restricted to models. Therefore, it is of interest to see, how well such models match the *ab initio* findings.

The determination of a model from the *ab initio* data separates into two steps. The first is the choice of the model space, i.e., which orbitals to include, and the computation of the relevant single-particle Hamiltonian. In the second step, the effective interactions are computed.

A. Relevant single-particle space and single-particle Hamiltonian

The information provided by the *ab initio* calculation concerns atomic orbital degrees of freedom, but so far, no more

delocalized degrees of freedom such as Wannier orbitals extending over sets of atoms. Models built from delocalized orbitals cannot be directly compared to the *ab initio* data but would need to be derived in a second step from models based on atomic orbitals.

The smallest model used for the high- T_c compounds based on atomic degrees of freedom is a three-band model, containing as atomic orbitals the $\text{Cu}3d_{x^2-y^2}$ and the $\text{O}2p_b$ orbitals. However, from the *ab initio* charge analysis (see Table II), one notes non-negligible fillings of $\text{Cu}4s,p$ and even deviation from complete filling for the $\text{O}2s$ orbitals. It is also known that the $\text{Cu}4s$ orbitals contribute actively to the band structure of the most relevant half-filled band. This was worked out before from LDA calculations.⁵¹ As a compromise, the selected model space for the present application is chosen to consist of $\text{Cu}3d_{x^2-y^2}$ and $4s$ and the $\text{O}2p_b$ orbitals. This model is also selected because an LDA equivalent exists.⁵¹

Note that these orbitals cannot be seen as a perfect representation of the corresponding *ab initio* orbitals. When taking the charge distribution for the SCF ground state from Table II, then the orbitals included in the model represent 4.84 electron per unit cell for the SCF ground state and 4.89 for the correlated ground state instead of 5.0 as they do for the half-filled band case in the model. Consequently, there can be no perfect agreement between such a four-band model and the real system.

Instead, the most relevant properties are to be matched. Here, the following properties are selected. The first is the half-filling of the uppermost band. This fixes the model charge at five electrons per unit cell. The second is the exact occupation of the $\text{Cu}3d_{x^2-y^2}$ orbital obtained from the respective *ab initio* calculation. Since the influence of particular correlations will be investigated, *ab initio* calculations with only partial inclusion of correlations and varying $\text{Cu}3d_{x^2-y^2}$ occupation will also be fitted. The third is the form of the Fermi surface. The model Fermi surface shall match the *ab initio* Fermi surface. This is important when longer-range correlations are concerned, and puts restrictive bounds on the $\text{Cu}4s$ occupation. A model $\text{Cu}4s$ occupation taken from the *ab initio* result would lead to a Fermi surface that deviates too strongly from nesting. Consequently, the $\text{Cu}4s$ model occupation is set to 0.25. The omitted $\text{Cu}4s$ charge in the *ab initio* calculation apparently stems from bands omitted in the model. Fixing the two other occupations freezes the $\text{O}2p$ occupation. It turns out that the deviation of the latter from complete filling is only half as large for the model as for the true ground state, indicating the bias and the limits of the four-band model.

Having determined the model occupations for a particular *ab initio* fit implicitly defines the diagonal or crystal-field terms e_i of the model. These e_i contain exchange and correlation contributions of the omitted degrees of freedom as well as exchange contributions due to the added on-site interactions of the model. Consequently, they differ for every fit. Each time, they are determined self-consistently for the model calculation so that the intended charge distribution is obtained.

The second set of parameters describes the delocalization of the electrons. It consists of the hopping terms. Here, it is assumed that the omitted external degrees of freedom have

no influence on these terms. Since only on-site interactions will be included, no nonlocal exchange contributions arise in the model. The hopping terms therefore represent the nondiagonal Hartree or alternatively, LDA matrix elements. There are only two relevant hopping parameters for this four-band model. From the LDA fit, it holds for the $3d,2p$ hopping, $t_{dp} = -1.6$ eV; and for the $4s,2p$ hopping, $t_{sp} = -2.3$ eV.⁵¹ At present, these hopping elements cannot be directly computed by the LA since CRYSTAL92 (Ref. 8) does not separate kinetic-energy (plus Hartree) terms from exchange terms. However, an estimate can be made. The Fock matrix elements, $f_{ij} = t_{ij} + V_{ij}(\text{exch})$, can be computed. For them, it is found that $f_{dp} = -2.8$ eV and $f_{sp} = -4.2$ eV. When approximately correcting for the exchange using the relation $V_{ij}(\text{exch}) \approx -(1/|\vec{R}_i - \vec{R}_j|)P_{ij}$, values of $t_{dp} = -1.7$ eV and $t_{sp} = -2.9$ eV result. The t_{pd} term equals the LDA value. This indicates that in the future hopping terms between orthogonalized atomic orbitals for models can be directly computed by the LA. On the other hand, the t_{sp} from the LDA fit is 20% smaller. This difference probably arises because the LDA fit accounts for the omission of the $4p$ orbitals, which otherwise would change the higher-energy band, while the estimates from the LA represent the original bare hopping. In the following, the LDA values for the hopping are taken.

The charge distribution of the original single-particle LDA model Hamiltonian [with the LDA values for the e_i (Ref. 51)] amounts to a $\text{Cu}4s$ occupation of 0.3, also strongly reduced due to the need for an adequate Fermi surface. The $\text{Cu}3d_{x^2-y^2}$ occupation for this model is 1.4, and apparently represents the $\text{Cu}3d_{x^2-y^2}$ contributions of the four included bands.

B. Interaction terms

For the determination of interaction terms in the model, correlation functions are available. In the model, only atomic or on-site interactions are included. These are the diagonal interactions for electrons in the same orbitals, U_{3d}, U_{4s}, U_{2p} and the interaction between the $\text{Cu}4s$ and $\text{Cu}3d_{x^2-y^2}$ orbitals on the same atom, $U_{4s,3d}$. These interactions are fitted on a one to one basis with the help of the corresponding on-site correlation functions.

The effective local model interactions U_i are indirectly generated from the long-range Coulomb interaction that prevails in the *ab initio* calculation. In this process, different kinds of rescaling occur. One rescaling process is called folding. It is a reduction that is not connected to screening. When reducing a single atomic fluctuation then not the original atomic interaction is measured but the difference between this interaction and the residual interaction of the electrons shifted in the process. For an almost empty band, the residual interaction is zero while in zeroth order, for a half-filled band, it is the neighbor interaction. A more detailed discussion was presented in Ref. 16. Another rescaling is due to screening effects, and here two sources exist. One is the degrees of freedom not included in the model, and the other is correlations also present in the model but not activated for the lack of a longer-range model interaction.

In the following we will add correlations stepwise to the *ab initio* calculation, and will stepwise interpret the *ab initio* result in terms of modified model interactions. This way, the

TABLE V. Effective on-site interaction parameters U_i (eV), as obtained in different approximations. The final estimate is also given in comparison to typical LDA results (Refs. 21–23, 53). The individual terms are explained in the text.

Correlations	U_d	U_s	U_{sd}	U_p		
On site, single without charge transfer	20.8	1.8	1.3	6.6		
On site, single	12.0	1.7	1.1	6.6		
On site, global	10.4	1.8	1.2	8.0		
CuO nn, global	8.8	1.8	1.1	7.6		
All, global	6.3	1.8	1.1			
Estimate	5.7	± 1.0	1.8	1.1	6.0	± 1.0
LDA	9.0	± 1.0			4.5	± 2.0

derivation of a local U from the bare Coulomb interaction can be quantitatively understood. The end product is local model interactions that represent the true ground state. The actual computation procedure for the model is as follows. The ground state for the single-particle part of the model Hamiltonian is easily obtained. It is used as an input into the LA program like the CRYSTAL92 results in the *ab initio* case. The correlation calculation is then performed by the LA program package, but with the interactions reduced to the model interactions. In principle, for the model, a set of calculations for different clusters would be necessary as in the *ab initio* case before. In reality, the fit was performed by matching only correlations in one, namely the largest cluster to the corresponding *ab initio* results. This cluster consists of five active Cu atoms and four active O atoms. Every model single-particle calculation and subsequent correlation calculation is embedded into a self-consistent cycle in which the respective single-particle energies e_i of the model are fixed so that the charge distribution of the particular correlated state of the model matches the *ab initio* counterpart.

When comparing model and *ab initio* correlations, an additional constraint needs to be taken into account. It is that correlation functions can only be directly compared when the respective occupations of the *ab initio* calculation and the model are identical. A similar constraint arises from the folding effect on the value of U . This is also strongly occupation dependent. While this poses no problem for the $\text{Cu}3d_{x^2-y^2}$ orbital, it involves the other two whose charges do not match. Therefore, interaction terms for these orbitals are determined in an intermediate step in which the model charge balance between the $\text{Cu}4s$ orbitals and the $\text{O}2p$ orbitals is shifted so that it agrees with the *ab initio* result for the momentarily treated atom. Fortunately, the different interactions do not influence each other much, so that no sizable ambiguity arises from this procedure. A test can be conducted by recomputing U_{3d} for the different choices. U_{3d} varies by less than 10%. It is largest for the highest $4s$ occupation because then the $4s,3d$ screening explicitly handled by the model itself is largest. For the other occupations, larger fractions of this screening are mapped by a reduced interaction parameter U_{3d} .

Sets of parallel calculations were performed in the following steps. First, correlations were introduced on a single atom only, once for Cu and once for O. In both cases atomic charge transfers were alternatively allowed or blocked to investigate their effect on U . The corresponding *ab initio* cal-

ulation was also restricted to correlations on single atoms only. This leads to unscreened effective interactions U when only single correlation operators each are included. These interactions U although unscreened are folded from the Coulomb interaction and no longer represent the original atomic interaction matrix elements. With charge transfer excluded, the results are given in the first line of Table V. Although folded, the U_{3d} is not very far from the atomic interaction matrix element, which is expected to be $U_{atom} \approx 25$ eV. The folded interaction U_{2p} on O on the other hand is quite small. It can be compared to similar interactions obtained before for the atomic orbitals on C compounds.¹⁶

The values for U_{4s} and $U_{4s,3d}$ are very small. The folding effect resulting from neighbor interaction contributions is expected to be, relatively speaking, largest for the latter terms because the $4s$ orbital is most extended. Also it should be remembered that the model contains effective $3d-4s$ hopping terms that are 20% smaller than the original values. For weak correlations it holds that correlations scale $\approx U/t$. Correcting for this renormalization would lead to a 25% enhancement of the U_{4s} . Finally, we recall that part of the *ab initio* $4s$ occupation apparently stems from other bands and might be involved in hopping processes in the *ab initio* calculation that are not represented in the model. Taking this into account should lead to an additional enhancement of U_{4s} . For comparison, the value for the effective local interaction in another system with $4s,4p$ electrons, namely, Ge, is 3.1 eV,¹¹ which is not too different from such a rescaled value.

The direct correlation between the $4s$ and the $3d$ orbitals on the Cu site when added has only a very small influence on the value of U_{3d} , and the value of the U_{4s} and $U_{4s,3d}$ is not very relevant for U_{3d} . This is unexpected. Similar interactions were important in earlier applications where the screening between π and σ electrons in C isomorphs or organic compounds was concerned.¹⁶ In these cases electrons in half-filled bands were screened by electrons in wider bands that were also half filled.

Next, local charge transfers are allowed that arise due to correlations. For the single Cu site, this is a charge transfer from the $3d$ into the $4s$ orbitals. It leads to a strong reduction for U_{3d} (see the second line in Table V). Partly, this reduction originates from the change in occupation itself because the folding reduction of the original atomic interaction due to longer-range Coulomb terms is largest for half-filled atomic

orbitals,¹⁶ and the change in Cu3d occupation is toward half-filling. The dominant contribution is from the 4s,3d screening. Such a screening was proposed by Herring long ago.⁵² Astonishingly, it comes into play with the help of a charge transfer when starting from the uncorrelated ground state, and the major role of the 4s orbitals is to represent a reservoir of states. This is interpreted in the following way. In HF approximation, the fluctuations are somewhat reduced by a too-large occupation as compared to that of the true ground state (see the discussion of the magnetovolume effect in Sec. III C). The correct occupation is then obtained by the added single-particle correlation operators. In this way fewer fluctuations are induced than would arise within an uncorrelated ground state that has the correct occupation. There are residual fluctuations, part of them from the original uncorrelated ground state, and part from the charge transfer due to single-particle correlation operators. These fluctuations are reduced with the help of the two-particle operators. In the model, a sizable part of the screening electrons is no longer included. When fixing the 3d occupation at the correct value, then much larger fluctuations arise for the model single-particle ground state than for the original *ab initio* uncorrelated ground state. With the original U_{3d} , a suppression of fluctuations for the model would result that is very much larger than the suppression of charge fluctuations due to two-particle correlation operators in the *ab initio* case. Consequently, a false description of the 3d correlation corrections would be made. When the reduction of fluctuations is adjusted to the known correction a very much reduced effective interaction U_{3d} is found.

This scenario for the 4s,3d screening is very different from the previously treated cases. As just mentioned, the screening of the electrons in the half-filled π bands in organic systems or C isomorphs due to the electrons in the half-filled σ bands was not at all connected with a charge transfer but originated solely from two-particle correlation operators, i.e., can be seen as a kind of classical screening.

For O, no on-site charge transfer effect, occurred. It is plausible that the only possible charge transfer, that is with the not completely filled 2s orbitals is marginal. In a subsequent calculation, all on-site correlations in the cluster were treated at once, and also charge transfer between the atoms was allowed. The result is displayed in the third line of Table V. There is an additional small charge transfer out of the Cu3d orbitals, leading to a small further reduction of U_{3d} . From this term on, the U_{3d} obtained for the minimal 4s occupation are given. Changing to this reduced value of the 4s occupation contributes a reduction of U_{3d} of 0.8 eV. This reduction arises because the residual 4s occupation is connected with a smaller screening. There is also a large charge transfer into the O2p orbitals. This causes a reduction of the folding effect and a sizable enhancement of U_{2p} . Remember that on this level only on-site correlations were included in the *ab initio* treatment. In particular, the long-range part of the Coulomb interaction was not screened at all. When nn Cu-O correlations are also included (line 4 of Table V), both model interactions are further reduced. The effect is larger for U_{3d} , where a charge transfer and screening come together, and smaller for U_{2p} , where a screening gain is reduced by another enhancement due to the inverse charge transfer. A sizable further reduction of U_{3d} occurs when all

correlations in the cluster are included. This is mostly due to the Cu-Cu spin correlations and the 3d,2p charge transfer caused by them. For U_{2p} , no value was computed for this case. A computation of U_{2p} requires a strong charging of the 4s orbital. In this particular case, it is so large that the 3d orbitals are overscreened. This means that even for sizably enhanced U_{3d} , too small correlation corrections of the 3d charge fluctuations were obtained. When keeping the original U_{3d} obtained for the other distributions, a value of $U_{2p} \approx 9$ eV was obtained. This represents a further enhancement due to the charge transfer into the O2p orbitals.

The values for the model interaction parameters obtained in this way can be seen as upper limits for the true model parameters. This is because only specific correlation corrections have been thus far included. Part of the excluded correlation corrections can be estimated. This is first the effect of the very short-range intra-atomic correlations. Their inclusion led to a reduction of the U by 10% or 0.5 eV for the C isomorphs.¹⁶ A similar reduction is expected for O. For Cu a somewhat larger reduction is expected due to the higher density and due to the screening influence of the filled 3s and 3p shells. Next is the omitted long range and polarization corrections. Such corrections are irrelevant for half-filling.¹⁶ Consequently, they should have no large effect on the U_{3d} . However, they should at least reduce a large fraction of the enhancement of U_{2p} with charging. The resulting estimate of the model parameters is given in the fifth line of Table V, together with a rough error estimate. Note that this is the first calculation of its kind for an ionic compound as well as for a metallic compound containing transition-metal atoms. Future applications will certainly reduce the uncertainties of the error estimates.

Values for the effective atomic interactions have been thus far computed by LDA frozen charge calculations. From these, an effective local interaction U is obtained that does not distinguish between different d orbitals and the total angular momentum of the atomic charge. In a second step, higher-order Slater parameters were added that are taken from experiments on atoms. An introduction is given in Ref. 53. Table V contains an average over LDA results^{21–23,53} for the resulting diagonal interaction of the $3d_{x^2-y^2}$ orbitals, U_{3d} , which here is identical to the diagonal interactions of the other 3d orbitals. Partially, those calculations also contained results for neighbor Coulomb interactions V (typically 1 eV or smaller). In such cases, the values presented in Table V are the differences $U_{3d} - V$. The LDA interaction is considerably larger than the one found from the LA calculation, and would result in too-large correlations if used for the model.

Note that the definition of U is totally different in the two approaches. The one (LDA) freezes charges and does not care for their dynamics, i.e., whether they are essentially localized or whether they are delocalized. Also, only the nearest-neighbor environment matters. So for CuO, almost the same interaction is obtained as for the high- T_c materials.⁵³ The other method (LA) maps all particular correlation effects even due to longer-range interactions of the delocalized electrons into an effective folded local interaction U . When looking for the derivation of the LA value, then it is seen that for the considered system, a very peculiar Cu neighbor interaction (or spin correlation) leads to a re-

duction of 2.5 eV below the LDA value. Such an effect is $3d_{x^2-y^2}$ specific and would not be expected to play a role for the other $3d$ orbitals. It would also not be expected for CuO for a lack of neighbor Cu coupling. For the latter compound, the U_{3d} of the LA are expected to be in the range of the LDA values.

The LDA results were used to explain photoemission experiments for different transition-metal compounds. Photoemission spectra calculated for an Anderson impurity model with the computed LDA values of $U_{3d}=9.5$ eV (Ref. 25) led to very good agreement with experiment for CuO and (with a particular exception) for Nd_2CuO_4 . A model when mapped to the same experiment led to a value of $U_{3d}=8.4$ eV for CuO.⁵⁴ This demonstrates that the LDA values are the correct values for the interactions among the completely localized $3d$ orbitals. However, this cannot be taken as evidence for the correctness of the value for the $3d_{x^2-y^2}$ orbitals. A modification of the latter interaction towards the LA result would probably not change the computed spectra very much. There is a small deficiency for Nd_2CuO_4 , though, when fitted to the LDA values. This is the existence of a local singlet peak at the upper band edge in the calculation, which also shows up in calculation and experiment for CuO, but not in the experiment for Nd_2CuO_4 . It is a valid speculation whether the reduced $3d_{x^2-y^2}$ U_{3d} originating from the effective neighbor Cu correlations in the plane would be sufficient to remove this deficiency.

The U_{2p} interaction of the LA is in qualitative agreement with earlier values found for the $2s,2p$ interactions in diamond [7.2 eV (Ref. 11)] but larger than the LDA estimate. There exists a spectroscopical fit for $U_{2p}=5.5$ eV.⁵⁵

The presented difference between the LA values and the LDA values of U_{3d} matches the difference between LDA and experiment found earlier for the transition metals. For the transition metals, the U_{3d} of the LDA are apparently independent of band filling^{56,57} while the experimentally needed quantities are strongly filling dependent and considerably smaller—except for the completely filled $3d$ band limit.^{17,18,16,19} It was proposed to resolve this discrepancy and the filling dependence of U_{3d} by a not fully screened neighbor interaction V . This would explain the LDA deviations and the filling dependency of U_{3d} as a folding effect.¹⁶

Calculations with the LA are now feasible for transition metals. The results obtained here give hope that from such calculations, appropriate values for the U_{3d} of the transition metals can be obtained. For comparison, the value of U_{3d} needed for Ni is 4.7 eV, and not very much lower than the final LA estimate for Cu in SrCuO_2 .

V. MODEL INTERACTION AND SPIN CORRELATIONS

The model interactions derived in the last section were optimized with respect to charge distribution and on-site correlations. Next, we will control how well this model is also able to reproduce the most interesting longer-range correlation features, namely, the spin correlations between different Cu $3d$ orbitals.

For the five Cu cluster, the results of the model calculation with $U_{3d}=6.3$ eV are compared to the corresponding *ab initio* values in Table VI. As can be seen, the model neighbor spin correlations are only half of the *ab initio* values, and the

TABLE VI. On-site and ν th neighbor Cu- $3d_{x^2-y^2}$ correlation functions for the cluster with five active Cu atoms. *Ab initio* results in comparison to model results with differing U_d .

Computation	Δ_{3d}	$\tilde{S}_i \tilde{S}_{i+\nu}$		
		$\nu=1$	$\nu=2$	$\nu=3$
<i>Ab initio</i>	-0.122	-0.140	0.075	0.072
$U_d=6.3$ eV	-0.122	-0.071	0.013	0.011
$U_d=7.8$ eV	-0.145	-0.097	0.025	0.024
$U_d=9.4$ eV	-0.160	-0.126	0.045	0.043

second-neighbor terms are reduced to one-sixth. Consequently, the four-band model with only on-site interactions included can not consistently reproduce on-site correlations and neighbor spin correlations. *Ab initio* neighbor spin-correlation functions are only matched by a U_{3d} that is 50% to large, and even then, the deficiency of the second-neighbor correlation functions is not completely removed (see Table VI).

Part of these discrepancies can be understood by considering the U dependence of the individual correlation functions calculated by means of the weak-correlation expansion. Here, the proximity to the magnetic instability plays a particular role. For the model (and for the *ab initio* calculation), the interaction enters in two quantities, namely, $\langle \text{OH} \rangle$ and $\langle \text{OHO} \rangle_c$. If the $\langle \text{OHO} \rangle_c$ were not depending on U , then the variational parameters (and the correlation functions up to saturation) would rise linearly with interaction strength. The model results are different and indicate that the interaction dependency of the second terms must come into play. This holds particularly true for the longer-range correlations, which rise very much more than linearly with interaction. This anomalous U dependency can only be understood by the proximity of the magnetic phase. As discussed before, the terms $\langle \text{OHO} \rangle_c$ represent the two-particle excitation energies. Close to a magnetic instability, these might become very much smaller and tend to zero, leading to an anomalous U dependence of the correlation parameters. Apparently, this applies to the model.

This interpretation also explains why the longer-range spin correlations in the model are relatively weaker than for the *ab initio* case. The diagonal terms of $\langle \text{OHO} \rangle_c$ represent energy differences of bare excitations out of the SCF ground-state wave function. This means that in the *ab initio* calculation, for these matrix elements the uncorrelated or HF susceptibility enters. In the model, however, the calculations were not performed with bare but with screened interaction parameters. This means that for the longer-range spin correlations the energy difference of bare excitations is computed with screened interactions and, therefore, contains correlations to some extent, in contrast to the *ab initio* calculation. Consequently, the model result for the longer-range spin correlations might be more adequate than the *ab initio* result and might even indicate by which amount the *ab initio* results need to be corrected. With only second- or third-neighbor correlations included, the model is still far from instability, in contrast to the conclusion derived from the *ab initio* calculation. A magnetic instability might only occur when considerably longer-range magnetic correlations are added. It

cannot even be excluded that the charge transfer connected with magnetic correlations causes a first-order phase transition, and that no divergence of the long-range correlations can be detected in the metastable state without broken symmetry.

Nearest-neighbor spin correlations do not display such a strong U dependence. While it cannot be excluded that the difference between *ab initio* and model results might also originate from the overestimated Stoner enhancement, there is another deficiency of the model that points to a different source. The neighbor spin correlations are connected to an explicit $\text{Cu}3d\text{-O}2p$ charge transfer that is smaller by almost one order of magnitude smaller in the model than in the *ab initio* calculation. A reason for this may be that the $\text{Cu}4s,p$ degrees of freedom are mostly removed from the model and only indirectly included in the form of reduced on-site interactions. It might well be that these omitted degrees of freedom contribute more actively to the neighbor-Cu-spin correlations with the help of an induced magnetic exchange interaction between neighbor Cu sites. Another reason for the discrepancy between *ab initio* and model results might be that the O occupation in the model is considerably larger than in the *ab initio* case, and might also reduce the charge transfer.

Apparently, the four-band model with on-site interactions only is not quite adequate to deal with the most interesting outcome of the *ab initio* calculations, namely, the anomalous neighbor spin correlations.

The Stoner enhancement in the longer-range spin correlation functions of the model calculation of the four- (or three-) band model and also apparently in the *ab initio* calculation is very different from results expected for a half-filled single-band Hubbard model. When using a weak-correlation expansion for the latter, then it is well known that for the one-dimensional case all interaction contributions in the terms $\langle \text{OHO} \rangle_c$ drop out. This means a linear rise of all correlations with U but no Stoner enhancement. For the two-dimensional model with perfect nesting, similar results are expected. It cannot be ruled out that closed loop terms lead to interaction contributions in the $\langle \text{OHO} \rangle_c$ for the nonnesting case but such terms are not yet present in the considered five-atom cluster. This indicates that the magnetism in the real system is essentially of itinerant or spin-density-wave nature (although strongly enhanced by the almost perfect nesting), and that a simple single-band Hubbard model might not be the correct approximate description.

VI. THE MODEL AWAY FROM HALF-FILLING

The computations performed so far were restricted to the so-called half-filled band case. As mentioned before, the program CRYSTAL92 can only be used for an integer number of electrons per unit cell. There is no such restriction for the LA program package. Consequently, the model calculations can easily be extended to partial fillings. For simplicity, the model SCF calculations were not repeated for differing fillings but the single-particle Hamiltonian at half-filling was frozen in, and only the Fermi energy was shifted. This approximate treatment seems justified because contributions relevant for charge redistribution such as the long-range

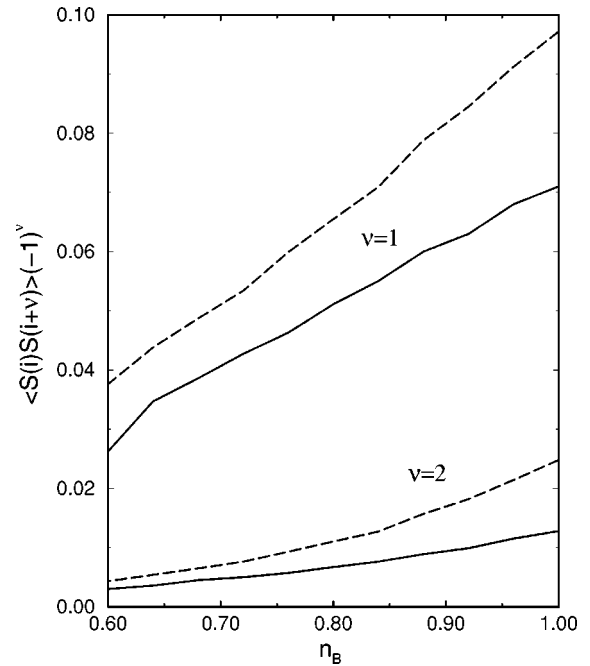


FIG. 2. Nearest-neighbor ($\nu=1$) and second-nearest-neighbor ($\nu=2$) spin correlation function in dependence of the filling n_B of the uppermost band, obtained for a model with $U_{3d}=6.3$ eV (continuous lines) or 7.8 eV (broken curve), respectively.

Madelung terms are not included in the simple on-site interaction model.

Of interest is the dependency of the neighbor and of the longer-range spin correlations on band filling. Figure 2 displays the nearest-neighbor ($\nu=1$) and next-nearest-neighbor ($\nu=2$) Cu-spin correlations as a function of the occupation of the uppermost band (n_B). These correlation functions were taken from calculations for a five-Cu-atom cluster again. Corrections towards the full results are typically 20 percent for the nearest-neighbor terms and more than 100% for the second-nearest-neighbor contributions. Two values for the interaction parameter U_{3d} were taken, namely the value deduced from the *ab initio* fit (6.3 eV, continuous lines), and a value enhanced by 20% (7.8 eV, dotted line). The second computation with an enlarged U_{3d} was made to obtain an estimate for the four-band-model shortcomings in comparison to the fictitious *ab initio* result.

Both correlation functions reduce in strength when electrons are removed. However for the range of interest, i.e., around optimal doping ($n_d \approx 0.8$), both functions are still sizable and not very much smaller than for the metastable nonmagnetic half-filled case. This *a posteriori* justifies the choice of such a metastable state in the *ab initio* correlation calculations. It also demonstrates that for all fillings of interest very sizable nearest-neighbor short-range antiferromagnetic correlations exist together with longer-range itinerant antiferromagnetic fluctuations. The U dependence of the longer-range correlation function is more pronounced and is strongest close to half-filling, indicating again the underlying Stoner enhancement.

Also of interest is the change of the charge distribution with doping. In the single-particle approximation, the electrons close to the Fermi surface are mostly d -like. Figure 3 displays the non- d -fraction of the density of states as a func-

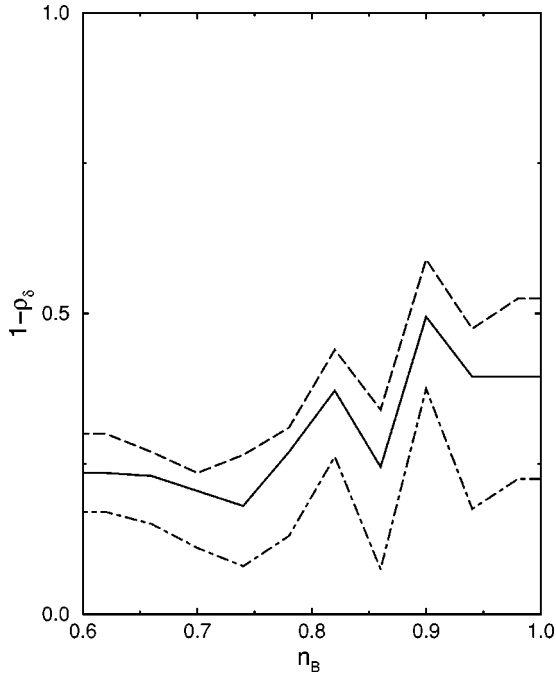


FIG. 3. Relative non-3d-like density of states at the Fermi energy in dependence of the filling n_b of the uppermost band, obtained without correlations (dotted-broken curve), for $U_{3d}=6.3$ eV (continuous lines) and 7.8 eV (broken curve), respectively.

tion of doping. It can be seen that close to the Fermi energy it amounts to 17%. As mentioned before, the model itself is unable to account for Madelung corrections that would certainly modify such an extreme density distribution of the removed charge. Also, a possible redistribution that would come in with the self-consistent computation is not included. However, we will discuss to what extent correlations lead to a redistribution of the removed charge. As can be seen from Fig. 3, there is indeed a sizable change of character of the removed density. Most of this is change into O2p character. Again, the computation is performed for two values of U_{3d} . The smaller value (6.3 eV) leads to a 20% charge redistribution while the larger value leads up to 50% corrections close to half-filling. Photoemission experiments not too far from the magnetic state found indeed that the electrons removed from the system were largely of O2p character.⁵⁸

VII. SPIN CORRELATIONS AND NEUTRON-SCATTERING RESULTS

In the *ab initio* calculation for the half-filled case, very strong antiferromagnetic neighbor Cu spin correlations in connection with a Cu-O charge transfer and with long-range antiferromagnetic polarizations were found. The subsequent model calculations have shown that the neighbor spin correlations are not restricted to the immediate vicinity of half-filling but exist for every filling.

This prediction can be tested by comparing the calculated results with quantitative magnetic neutron measurements. From these experiments, a quasi-equal-time spin-correlation function $S(\vec{Q})$ was obtained⁷ for the metallic compound $\text{La}_{0.85}\text{Sr}_{0.15}\text{Cu}_2\text{O}_4$ by extending the energy integration up to 0.45 eV. The data show a strong longer-range structure that

is expected to exist independently of an also found small quasielastic scattering arising from an incommensurate spin density wave present in this particular compound. In the following, a comparison is made between the theoretical equal-time correlation function and the measured quantity. Both are not identical. The theoretical quantity is obtained for the infinite layer case where for 0.15 holes per unit cell apparently no incommensurate spin wave exists, and consequently less magnetic scattering is expected than for the measured compound. On the other hand, the theoretical quantity represents the true equal-time correlation function and contains contributions that are not in the range of the measurement.

The limiting equal time case of the measured correlation function is defined as

$$S(\vec{Q}) = \frac{1}{N} \int d^3\vec{r} \int d^3\vec{r}' S(\vec{r}, \vec{r}') e^{i\vec{Q}(\vec{r}-\vec{r}')}. \quad (21)$$

The theoretical spin-correlation function is derived from the model calculation at appropriate doping. It is represented by spin correlations between different orthogonal orbitals,

$$S(i, j, \vec{G}) = \langle \Psi_{\text{corr}} | \vec{s}_i(0) \vec{s}_j(\vec{G}) | \Psi_{\text{corr}} \rangle. \quad (22)$$

Here i denotes the i th orbital in the unit cell with atom position \vec{r}_i , \vec{G} represents the lattice vectors, and $\vec{s}_i(\vec{G})$ represents the spin operator for orbital i in the \vec{G} unit cell. When assuming that the spatial density distribution is shrunk to the nuclear positions,

$$S(\vec{r}, \vec{r}') \approx \sum_{i, j, \vec{G}, \vec{G}'} \delta(\vec{r} - \vec{r}_i + \vec{G}) \times \delta(\vec{r}' - \vec{r}_j + \vec{G} + \vec{G}') S(i, j, \vec{G}'), \quad (23)$$

one obtains

$$S(\vec{Q}) = \sum_{i, j, \vec{G}} S(i, j, \vec{G}) e^{i\vec{Q}(\vec{r}_i - \vec{r}_j - \vec{G})}. \quad (24)$$

This function is very easy to compute. Figure 4 contains the results for a particular \vec{Q} direction, namely, the diagonal (1,1) axis, obtained in different approximations. The zone boundary is at $h=1$, the intensity is given per formula unit, which here is equivalent to a unit cell or to a single Cu atom.

The lowest curve represents the result for the single-particle ground state. It represents the exchange holes. As the finite value at $h=0$ indicates, the summation in Eq. (24) was not brought to convergence. Instead, the Cu-Cu density-matrix elements were only included up to the fourth neighbor, and no density-matrix elements with 4s or 2p orbitals extending beyond the nearest-neighbor Cu-O terms were added. The maximal deviation occurs for $h=0$, where the contributions from all missing terms add up. Due to dephasing, the correction is very much smaller for finite h . Due to the fine structure in the unit cell, this function is finite at the first lattice vector ($h=2$). This represents the Cu-O correlation function.

Next, short-range correlations as they are deduced from a single coherent five Cu cluster calculation are included (lower continuous curve). Here, the nearest-neighbor Cu-Cu correlations come into play and cause a peak at the zone

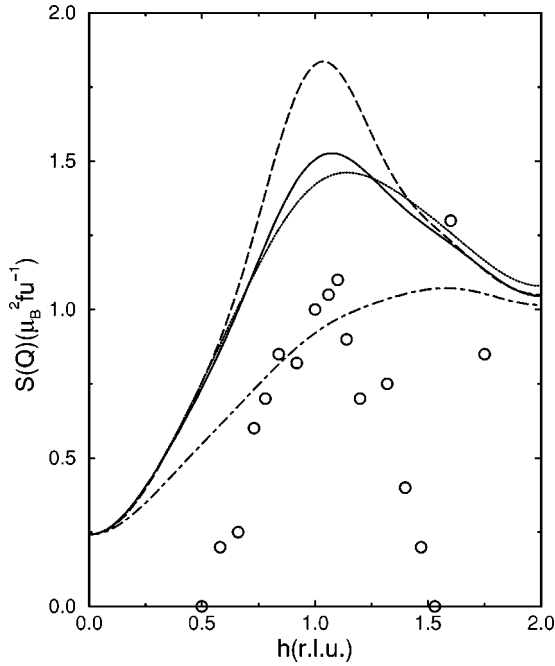


FIG. 4. Equal-time spin-correlation function $S(\mathbf{Q})$ for $\vec{Q} = (h, h, 0)$ in comparison to experiment (Ref. 7) (empty circles). Given are the results of the HF ground state (broken-dotted curve), the five-atom cluster result (lower continuous curve), and the nine-atom cluster result (upper continuous curve) for $U_{3d} = 6.3$ eV, and the nine-atom cluster result for $U_{3d} = 7.8$ eV.

boundary ($h = 1$). When extending the correlation treatment to a nine Cu cluster, second- and third-neighbor correlations are more correctly treated. They lead to a narrowing of the peak and to a small enhancement (upper continuous curve). Finally, the corresponding values with enlarged U (7.8 eV instead of 6.3 eV) are also given (broken curve). Increasing U leads to a strong enhancement of the maximum, indicating again the proximity to a magnetic phase transition. These results are compared to experiment⁷ (dots) in Fig. 4. As expected, the theoretical equal-time correlation function the energy integration of which extends only to 0.45 eV. Beyond $h = 1.5$, the experimental results are influenced by the next Bragg peak, and are no more meaningful.

There are specific contributions to the theoretical correlation function that are not expected to be seen by experiment. These are the short-range contributions connected with the Cu-O hopping, arising already without correlations. The hopping energy connected with this part of the correlation function is $t = 1.6$ eV, and very much larger than the energy cut-off. Consequently, only a marginal part of these contributions is expected to show up in experiment. A considerably larger fraction of the uncorrelated longer-range Cu-Cu contributions is expected to show up since these mostly arise from the uppermost band. Also, the relevant correlation contributions are expected to be measured by experiment. While the on-site correlation functions might not fully show up, the effect of the neighbor Cu-Cu spin correlations is expected to arise mostly from the electrons in the uppermost band, and the longer-range enhanced spin correlations are certainly connected with electrons close to the Fermi surface, as is indicated by their strong resonance de-

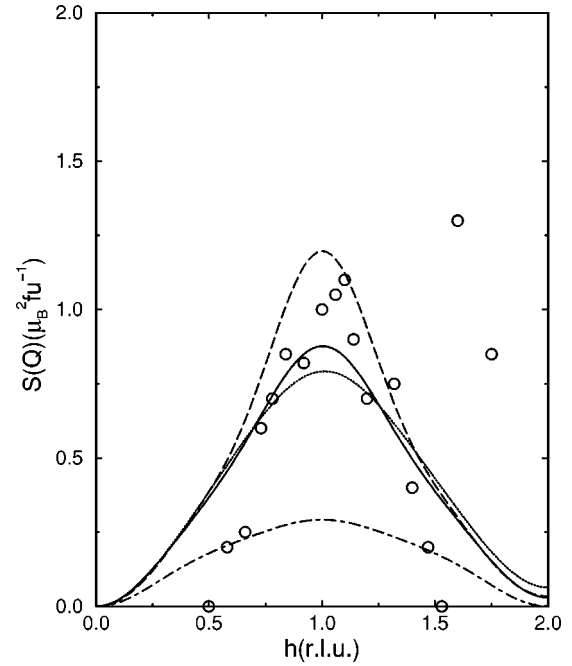


FIG. 5. Cu-Cu-dependent part of the equal-time spin-correlation function $S(\mathbf{Q})$ in comparison to experiment. Definition of the curves as in Fig. 4.

pendence on U . Figure 5 displays the correlation functions of Fig. 4, but with all Cu-O contributions of the single-particle approximation removed, and with the residual function shifted so that $S(0) = 0$ holds. The residual Cu-Cu single-particle contributions are small and essentially bell shaped (lowest curve). The correlation contributions lead to a pronounced maximum around the zone boundary. When correlations resulting from the nine Cu cluster calculation are included, then the half-width of the correlation peak corresponds well to the half-width of the experimental peak. However, for the value of U taken from the fit to on-site correlations, the integrated scattering intensity is not larger than the experimental counterpart. The result for a 20 percent enhanced U finally leads to a correlation function that is systematically larger than the experimental curve. The *ab initio* calculation if performed for the relevant doping would certainly give a correlation function as large as or even somewhat larger than the model result for the enhanced interaction. A future comparison with experimental results for a metallic compound without a spin-density wave will allow us to decide whether the model results or the *ab initio* results are more reliable. The *ab initio* calculations might overestimate the Stoner enhancement, while the model might well leave out relevant degrees of freedom, and might consequently need to be extended.

The theoretical results represent not only the particular doping of 0.15 holes but should be representative for a wider range of doping even farther away from the magnetic case. As Fig. 2 demonstrates, the neighbor correlations that represent the weight of the peak around the zone boundary reduce only slowly with further doping. The longer-range correlations are expected to reduce faster, so that a continuous widening of the peak with further doping is expected. These correlation features appear over a rather wide range of dop-

ing and have consequently, no direct connection with any kind of Mott-Hubbard transition.

The equal-time spin-correlation function was computed earlier for a one-band Hubbard model^{59,60} or for a t - J model.⁶¹ In these computations, due to the particular Fermi surface, at 0.15 doping a spin-density wave shows up. The resulting equal-time correlation function is different from the one given in Fig. 4. It is close to the bell-shaped curve of the uncorrelated electrons in Fig. 5 but enhanced by a factor of 3. In addition, for magnetically ordered states, there is a very narrow peak just at $h = 1.0$ (or a set of two peaks close to this point). This peak disappears for the not ordered states, but its width is usually not resolved due the finite k -point mesh used in these computations. There is no evidence for strong shorter- or longer-range spin-correlation features in the non-magnetic metallic state. This indicates that single-band models with local interactions do not adequately describe the low-energy degrees of freedom of the metallic case.

The extended range of longer-range antiferromagnetic correlations found in the *ab initio* calculation but also for the four-band model, contrasts with single-band model results. This is connected to the following difference. On-site correlations are strongest for a $3d_{x^2-y^2}$ occupation of 1. This occupation occurs at 0.4 to 0.5 doping. Antiferromagnetic order, on the other hand, is strongest for perfect nesting in the half-filled band case. Between both points, a region of strong fluctuations is found. For a single-band model, these different points are reduced to a single point, half-filling.

VIII. CONCLUSIONS

The results obtained within the framework of the LA can be hierarchically classified into the following categories. The first concerns the general field of *ab initio* calculations for the transition metals, the next deals with the connection of full Hamiltonian and model Hamiltonians, and the last one finally covers the specific electronic properties of the high- T_c compounds.

Concerning the general field of *ab initio* calculations for transition metals, we have presented the first LA computation, which also provides detailed correlation functions, and which, as mentioned is not connected to a homogeneous-electron-gas-like approximation. We could explicitly investigate those correlation effects that are out of the reach of the LDA. An example relevant for the general field is the correlation induced $3d$ - $4s$ charge transfer. A similar charge transfer is expected from magnetic order in the transition metals and was proposed long ago by Lang and Ehrenreich as an explanation for the inverse magnetovolume effect in Ni.³⁷ This can now be quantitatively addressed.

We have found that the weak-correlation expansion in which the LA is computed can be successfully applied to systems as strongly correlated as the high- T_c materials. Astonishingly, problems arose neither in the context of strong atomic correlations nor due to a possible Mott-Hubbard transition on either the atomic or a more extended unit-cell scale, but only from the closeness of the ground state to a magnetic phase and from the resulting Stoner enhancement. A future extension of this weak-correlation expansion, from the linearized to the full CCSD equations in the restricted operator space should help to reduce the latter problems.

The calculations have also demonstrated how important it is to use an SCF calculation for the full solid as a starting point. In the past, it has been necessary to restrict oneself to calculations for small Cu-O clusters when applications based on *ab initio* treatments beyond a homogeneous-electron-gas-based approximation were made. One of the first such calculations has also been done in the framework of the LA,³⁴ and a comparison of the results clearly shows how adversely cluster constraints influence basic results like the electronic charge distributions or correlation functions.

Concerning the transition from the *ab initio* calculation to a model Hamiltonian, the dominant issue is the determination and the analysis of the interaction parameters of the effective Hubbard models. Among others, we have provided a detailed derivation of the effective $\text{Cu}3d_{x^2-y^2}$ -interaction parameters, starting from the bare Coulomb interaction, and analyzed, in particular, the screening effect of the $4s,4p$ electrons that had been proposed long ago by Herring.⁵² A surprising finding was that this screening is not much connected with the residual interactions between the $3d$ and the $4s,4p$ electrons, but largely mediated by a charge transfer from the $3d$ orbitals into the $4s,4p$ orbitals, when starting from the SCF ground state.

The obtained $\text{Cu}3d_{x^2-y^2}$ -interaction parameter turned out to be somewhat smaller than the global $\text{Cu}3d$ interaction parameters that were determined by frozen charge LDA calculations. The difference apparently results from residual interactions between electrons in $3d_{x^2-y^2}$ orbitals on neighbor-Cu sites that are only accounted for when correlation functions are used as a means to determine the interaction parameter. A similar deviation was noted earlier for the case of the transition-metal interaction parameters, for which somewhat smaller values were obtained from fits to experiment than from computations by the LDA.¹⁶

Finally, we will address the specific properties of the metallic CuO compounds. On the single-electron level, our results are similar to the LDA results. This concerns, in particular, the relevance of the $4s$ orbitals for the dispersion of the half-filled band and for the form of the Fermi surface. However, there are also differences. Surprising is the one for the $3d$ occupation that comes out too large in the LDA. Furthermore, we found sizable correlations on different length scales. While the strong atomic correlations were expected for these compounds, we found in addition a strong magnetic nearest-neighbor Cu-Cu correlation that might even lead to a neighbor attraction of electrons with different spin. This correlation is not due to the longer-range magnetic fluctuations; however, it may well be enhanced by it. It is also connected with a sizable Cu-O charge transfer. A homogeneous-electron-gas-based method such as the LDA is expected to be able to handle neither such a correlation nor the connected charge transfer. This explains the just-mentioned difference in the $3d$ occupation. In addition, a sizable long-range magnetic polarization was found that can best be described in terms of a Stoner enhancement. All these features turn out to be present over a large doping range, and not only very close to half-filling.

The connection between variations in the magnetic correlations and the charge transfer is expected to result in interesting couplings between the magnetic and lattice degrees of freedom. In particular, it should not be surprising if the mag-

netovolume effect for the case of the half-filled-band systems turns out to be very small or even negative, as is the case in Ni.

The just-mentioned particular neighbor spin correlations, enhanced by longer-range magnetic fluctuations, dominate the spin-correlation function, and explain the features found in the measured spin correlations for $\text{La}_{0.85}\text{Sr}_{0.15}\text{Cu}_2\text{O}_4$.⁷ Apparently, neither the single-band-Hubbard model results nor the t - J -model results can explain this spin correlation function (see discussion in Sec. VII). It was not even possible to bring the results of the four-band model with only on-site interactions to good agreement with the *ab initio* results, where on-site and longer-range correlations were jointly concerned. It seems that a proper description of the real system can only be obtained if in such a four-band model the background-induced magnetic Cu neighbor interactions are explicitly taken into account, or if the model is generalized by an explicit inclusion of the $4p$ orbitals, perhaps even of

the full screening process of the $3d$ interactions by the $4s, 4p$ orbitals. In our future work, we shall investigate such extensions.

To conclude, *ab initio* correlation calculations can now be performed for the transition metals. With the local ansatz, details of the correlation functions as well as a good understanding of the relevant short-range correlation features can be obtained. The first application for a metallic high- T_c compound shows a fairly good agreement between the computed and the measured magnetic correlation functions.

ACKNOWLEDGMENTS

Thanks are due to C. J. Mei for making available the input files of his earlier calculations, and in particular to G. Zwicknagl, B. Farid, and O. Gunnarsson for a careful reading of the manuscript.

-
- ¹P. Hohenberg and W. Kohn, Phys. Rev. **136**, 864 (1964).
²W. Kohn and L. J. Sham, Phys. Rev. **149**, 1133 (1965).
³W. Pickett, Rev. Mod. Phys. **61**, 433 (1989).
⁴E. Dagotto, Rev. Mod. Phys. **66**, 763 (1994).
⁵G. Stollhoff and P. Fulde, J. Chem. Phys. **73**, 4548 (1980).
⁶G. Stollhoff, J. Chem. Phys. **105**, 227 (1996).
⁷S. M. Hayden, G. Aeppli, H. A. Mook, T. G. Perring, T. E. Mason, S.-W. Cheong, and Z. Fisk, Phys. Rev. Lett. **76**, 1344 (1996).
⁸R. Dovesi, V. R. Saunders, and C. Roetti, *Crystal92, User Documentation* (University of Torino, Torino, 1992).
⁹R. Jastrow, Phys. Rev. **98**, 1479 (1955).
¹⁰G. Stollhoff and M. Häser, Phys. Rev. B **45**, 13 703 (1992).
¹¹R. Pardon, J. Gräfenstein, and G. Stollhoff, Phys. Rev. B **51**, 10 556 (1995).
¹²M. V. Ganduglia-Pirovano and G. Stollhoff, Phys. Rev. B **44**, 3526 (1991).
¹³G. König and G. Stollhoff, Phys. Rev. Lett. **65**, 1239 (1990).
¹⁴G. Stollhoff, A. B. Pisanty, and M. Causa (unpublished).
¹⁵A. Heilingbrunner and G. Stollhoff, J. Chem. Phys. **99**, 6799 (1993).
¹⁶G. Stollhoff, Europhys. Lett. **30**, 99 (1995).
¹⁷A. M. Oleś and G. Stollhoff, Phys. Rev. B **29**, 314 (1984).
¹⁸G. Stollhoff, A. M. Oleś, and V. Heine, Phys. Rev. B **41**, 7028 (1990).
¹⁹D. v. d. Marel and G. A. Sawatzky, Phys. Rev. B **37**, 10 674 (1988).
²⁰G. Stollhoff, Europhys. Lett. **29**, 463 (1995).
²¹A. K. McMahan, R. M. Martin, and S. Satpathy, Phys. Rev. B **38**, 6650 (1988).
²²E. B. Stechel and D. R. Jennison, Phys. Rev. B **38**, 4632 (1988).
²³M. S. Hybertsen, M. Schlüter, and N. E. Christensen, Phys. Rev. B **39**, 9028 (1989).
²⁴J. Zaanen, O. Jepsen, O. Gunnarsson, A. T. Paxton, O. K. Andersen, and A. Svane, Physica C **153-155**, 1636 (1988).
²⁵O. Gunnarsson, O. Jepsen, and Z.-X. Shen, Phys. Rev. B **42**, 8707 (1990).
²⁶P. Horsch and W. Stephan, in *Interacting Electrons in Reduced Dimensions*, edited by D. Baeriswyl and D. J. Campbell (Plenum, New York, 1989), p. 341.
²⁷R. Wehl, C. O. Rodriguez, and M. Weissmann, Physica C **223**, 339 (1994).
²⁸A. Schäfer, H. Horn, and R. Ahlrichs, J. Chem. Phys. **97**, 2571 (1992).
²⁹This basis is implemented in the Turbomole basis input part; R. Ahlrichs, M. Bär, M. Häser, H. Horn, and C. Kölmel, Chem. Phys. Lett. **162**, 165 (1989).
³⁰P. J. Hay and W. R. Wadt, J. Chem. Phys. **82**, 270 (1985).
³¹C. J. Mei and V. H. Smith, Physica C **209**, 389 (1993).
³²J. Čížek, and J. Paldus, Int. J. Quantum Chem. **3**, 149 (1969); **5**, 359 (1971).
³³G. Stollhoff and A. Heilingbrunner, Z. Phys. B **83**, 85 (1991).
³⁴C. J. Mei and G. Stollhoff, Phys. Rev. B **43**, 3065 (1991).
³⁵G. Stollhoff and P. Thalmeier, Z. Phys. B **43**, 13 (1981).
³⁶H. Tange and T. Tokunaga, J. Phys. Soc. Jpn. **27**, 554 (1969).
³⁷N. D. Lang and H. Ehrenreich, Phys. Rev. B **168**, 605 (1968).
³⁸R. Dovesi, V. R. Saunders, C. Roetti, M. Cavasà, N. M. Harrison, R. Orlando, and E. Aprà, *CRYSTAL95 Users Manual* (University of Torino, Torino, 1996).
³⁹K. K. Smith and K. D. Jordan, J. Chem. Phys. **82**, 873 (1985).
⁴⁰C. W. Bauschlicher, H. Porridge, and S. P. Walch, J. Chem. Phys. **76**, 1033 (1982).
⁴¹R. C. Martin and P. J. Hey, J. Chem. Phys. **75**, 4539 (1981).
⁴²K. Karlsson, O. Gunnarsson, and O. Jepsen, Phys. Rev. B **45**, 7559 (1992).
⁴³O. Jepsen (private communication).
⁴⁴J. F. Janak and A. R. Williams, Phys. Rev. B **14**, 4199 (1976).
⁴⁵R. O. Jones and O. Gunnarsson, Rev. Mod. Phys. **61**, 689 (1989).
⁴⁶S. Fahy, X. W. Wang, and S. G. Louie, Phys. Rev. B **42**, 3503 (1990).
⁴⁷D. M. Ceperley and L. Mitas, Adv. Chem. Phys. **1**, 93 (1996).
⁴⁸O. K. Andersen, O. Jepsen, A. J. Lichtenstein, and I. I. Mazin, Phys. Rev. B **49**, 4145 (1994).
⁴⁹E. Manousakis, Rev. Mod. Phys. **63**, 1 (1991).
⁵⁰M. J. Jurgens, P. Burlet, C. Vettier, L. P. Regnault, J. Y. Henry, J. Rossat-Mignod, H. Noel, M. Po'tel, P. Gougeon, and J. C. Levet, Physica B **156-157**, 846 (1989).

- ⁵¹O. K. Andersen, A. J. Liechtenstein, O. Jepsen, and F. Paulsen, J. Phys. Chem. Solids **56**, 1573 (1995).
- ⁵²C. Herring, in *Magnetism, a Treatise on Modern Theory and Materials*, edited by G. T. Rado and H. Suhl (Academic Press, New York, 1973), Vol. IV.
- ⁵³A. K. McMahan, J. F. Annett, and R. M. Martin, Phys. Rev. B **42**, 6268 (1990).
- ⁵⁴H. Eskes, L. H. Tjeng, and G. A. Sawatzky, Phys. Rev. B **41**, 288 (1990).
- ⁵⁵H. Eskes, Doctoral thesis, University of Groningen, Groningen, 1992.
- ⁵⁶V. I. Anisimov and O. Gunnarsson, Phys. Rev. B **43**, 7570 (1991).
- ⁵⁷V. Drchal, O. Gunnarsson, and O. Jepsen, Phys. Rev. B **44**, 3518 (1991).
- ⁵⁸J. Fink, N. Nücker, E. Pellegrin, H. Romberg, M. Alexander, and M. Knopfer, J. Electron Spectrosc. Relat. Phenom. **66**, 395 (1994).
- ⁵⁹N. Furukawa and M. Imada, J. Phys. Soc. Jpn. **61**, 3331 (1992).
- ⁶⁰A. Moreo, D. J. Scalapino, R. Sugar, S. White, and N. Bickers, Phys. Rev. B **41**, 2313 (1990).
- ⁶¹A. Moreo, E. Dagotto, T. Jolicoeur, and J. Riera, Phys. Rev. B **42**, 6283 (1990).